

University of Dundee

## Retinal Imaging in Alzheimer's Disease

Cheung, Carol Y.; Mok, Vincent; Foster, Paul J.; Trucco, Manuel; Chen, Christopher L. H.; Wong, Tien-Yin

*Published in:*  
Journal of Neurology, Neurosurgery and Psychiatry

*DOI:*  
[10.1136/jnnp-2020-325347](https://doi.org/10.1136/jnnp-2020-325347)

*Publication date:*  
2021

*Document Version*  
Peer reviewed version

[Link to publication in Discovery Research Portal](#)

### *Citation for published version (APA):*

Cheung, C. Y., Mok, V., Foster, P. J., Trucco, M., Chen, C. L. H., & Wong, T-Y. (2021). Retinal Imaging in Alzheimer's Disease. *Journal of Neurology, Neurosurgery and Psychiatry*. <https://doi.org/10.1136/jnnp-2020-325347>

### **General rights**

Copyright and moral rights for the publications made accessible in Discovery Research Portal are retained by the authors and/or other copyright owners and it is a condition of accessing publications that users recognise and abide by the legal requirements associated with these rights.

- Users may download and print one copy of any publication from Discovery Research Portal for the purpose of private study or research.
- You may not further distribute the material or use it for any profit-making activity or commercial gain.
- You may freely distribute the URL identifying the publication in the public portal.

### **Take down policy**

If you believe that this document breaches copyright please contact us providing details, and we will remove access to the work immediately and investigate your claim.

## Retinal Imaging in Alzheimer's Disease

Carol Y. Cheung, PhD,<sup>1</sup> Vincent Mok, MD, FRCP,<sup>2</sup> Paul J. Foster, PhD, FRCOphth,<sup>3</sup> Emanuele Trucco, PhD,<sup>4</sup> Christopher L. H. Chen, BMBCh, FRCPE,<sup>5,6</sup> Tien Y. Wong, MD, PhD<sup>7,8</sup>

1. Department of Ophthalmology and Visual Sciences, The Chinese University of Hong Kong, Hong Kong,
2. Gerald Choa Neuroscience Centre, Therese Pei Fong Chow Research Centre for Prevention of Dementia, Lui Che Woo Institute of Innovative Medicine, Department of Medicine and Therapeutics, The Chinese University of Hong Kong, Hong Kong
3. National Institute for Health Research Biomedical Research Centre, Moorfields Eye Hospital NHS Foundation Trust NHS Foundation Trust and UCL Institute of Ophthalmology, London, UK
4. VAMPIRE project, Computing, School of Science and Engineering, University of Dundee, Dundee, UK
5. Memory Aging and Cognition Centre, National University Health System, Singapore
6. Department of Pharmacology, National University of Singapore, Singapore
7. Singapore Eye Research Institute, Singapore National Eye Centre, Duke-NUS Medical School, National University of Singapore, Singapore
8. Ophthalmology and Visual Sciences Academic Clinical Programme, Duke-NUS Medical School, Singapore

**Number of references:** 59

**Abstract count:** 162

**Word count:** 6,997

Review for JNNP

**Corresponding Author:**

Carol Y. Cheung, PhD

Email: [carolcheung@cuhk.edu.hk](mailto:carolcheung@cuhk.edu.hk)

Address: Department of Ophthalmology and Visual Sciences, The Chinese University of Hong Kong, 4/F Hong Kong Eye Hospital, 147K Argyle Street, Kowloon, Hong Kong SAR; T: +852 3943 5831 / F: +852 2715 9490

## **ABSTRACT**

Identifying biomarkers of Alzheimer's Disease (AD) will accelerate the understanding of its pathophysiology, facilitate screening and risk stratification, and aid in developing new therapies. Developments in non-invasive retinal imaging technologies, including optical coherence tomography (OCT), OCT-angiography and digital retinal photography, have provided a means to study neuronal and vascular structures in the retina in people with AD. Both qualitative and quantitative measurements from these retinal imaging technologies (e.g. thinning of peripapillary RNFL, inner retinal layer, and choroidal layer, reduced capillary density, abnormal vasodilatory response) have been shown to be associated with cognitive function impairment and risk of AD. The development of computer algorithms for respective retinal imaging methods has further enhanced the potential of retinal imaging as a viable tool for rapid, early detection and screening of AD. In this review, we present an update of current retinal imaging techniques and their potential applications in AD research. We also discuss the newer retinal imaging techniques and future directions in this expanding field.

## 1. Introduction

Alzheimer's disease (AD), the most common form of dementia, is a major public health and clinical challenge globally.<sup>1</sup> Despite decades in research, the pathophysiology of AD remains unclear. The current thinking is that the neuropathology of AD, as characterised by accumulation of misfolded amyloid- $\beta$  and tau protein, begins years before the onset of clinical symptoms. Given this long natural history, there are opportunities for early disease detection and thus timely intervention.<sup>2,3</sup> Indeed, recent clinical trials have suggested the efficacy of certain measures (e.g. lifestyle interventions or medication) in improving symptoms or slowing progression of AD.<sup>4</sup>

The definition of AD has also evolved in the past decade with the discovery of novel *in vivo* biomarkers for AD.<sup>5,6</sup> It has been shown that clinically diagnosed cases of dementia presumably due to AD may be amyloid-negative in up to 25% of cases.<sup>7,8</sup> Thus, biomarker confirmation has been proposed to improve the precision of AD diagnosis and now even biomarkers are indispensable for an AD diagnosis.<sup>9-11</sup> The evolution in definition and diagnostic criteria of AD and other dementias may account for some of the variations and differences seen between studies discussed in this review. The 2018 National Institute on Aging and Alzheimer's Association Research Framework defines AD *in vivo* by abnormal biomarkers of cerebral amyloid- $\beta$  deposition and pathologic tau and treats cognitive impairment as a symptom or sign of the disease.<sup>9</sup> This implies the cognitive function of a person affected by AD can thus range from cognitively unimpaired (preclinical AD), to mild cognitive impairment (MCI) (AD MCI), to dementia (AD dementia).<sup>9</sup> Although this latest framework encourages *in vivo* detection and study of AD at an earlier stage (e.g. preclinical AD or AD MCI), current technologies to detect amyloid- $\beta$  and tau pathology using positron emission tomography (PET) brain imaging or cerebrospinal fluid (CSF) examination are limited due to their high cost, technical complexity, invasiveness of

the procedures, and/or the necessity of using radioactive tracers. Thus, identifying alternative, more accessible technologies and biomarkers of pre-clinical AD prior to onset of cognitive impairment may accelerate the understanding of the pathogenesis of AD, facilitate screening and stratification of risk, and ultimately aid in the discovery, development and testing of new treatments or preventive therapies in clinical trials.<sup>3</sup>

The retina, a neurosensory layered tissue lining the back of the eye and directly connected to the brain via the optic nerve, receives light that the lens has focused, converts the light into neural signals, and sends these signals on to the brain for visual recognition. The retina has long been considered a “platform” to study disorders in the central nervous system (CNS), as it is an accessible extension of the brain in terms of embryology, anatomy and physiology (**Box 1**).<sup>12</sup> **Figure 1**. shows the optic nerve head, macular area, nerve fiber layer, arterioles and venules captured from a retinal photograph. Similar to the neurovascular unit (NVU) in the CNS, the retinal NVU contains neurons (ganglion cells, amacrine cells, horizontal and bipolar cells), glial cells (Müller cells and astrocytes) and vascular cells (endothelial cells and pericytes).<sup>13</sup> Evidence of retinal involvement in AD dementia has been shown in histopathological studies of *postmortem* specimens.<sup>14,51</sup> Associations of AD dementia with common eye diseases with overt clinical signs, such as age-related macular degeneration (AMD), diabetic retinopathy (DR) and glaucoma, have also been reported. In addition to digital retinal photography (**Figure 1**), recent advances in non-invasive retinal imaging technologies allow more detailed interrogation of the different retinal layers, and even deeper structures beyond the retina, such as the choroid including the choroidal vasculature. These retinal imaging technologies which include optical coherence tomography (OCT) (**Figure 2**) and OCT-angiography (OCT-A) (**Figure 3**), have provided researchers with further access to detailed retinal neuronal structure (e.g. nerve fiber layer, ganglion cell layer and

inner-plexiform layer) and microvasculature (e.g. foveal avascular zone), respectively. **Table 1** shows a glossary of retinal imaging technologies and parameters used in studying AD. Details of these technologies are summarized in **Supplementary Section 1**. In comparison to brain imaging technology, retinal imaging has the advantages of being non-invasive, comparatively low cost, increasingly widely available in non-tertiary (e.g. primary care and community) settings, and having different variables for quantifying the structures of retina. The development of next generation computational techniques such as artificial intelligence (AI) and deep learning (DL) algorithms have further enhanced the potential of data rich retinal imaging as a promising tool and a source of biomarker for AD, particular for individuals at preclinical AD stage. However, most of the retinal imaging technologies are still specialized equipment and the interpretation of data requires expertise from ophthalmologists or visual scientists.

In this review, we present an update of the current retinal imaging technologies, recent research findings, and future research applications in the study of AD.

## **2. Common Eye Diseases and AD**

Vision itself may be an important stimulus for the maintenance of cognitive health or reflect possible relationships between AD with underlying eye diseases.<sup>S2-S7</sup> Population-based and clinical studies have consistently shown that visual impairment<sup>S8-S14</sup> and a range of common eye diseases<sup>S15-S19</sup> are associated with dementia and impaired cognitive function. For example, in one study, older persons with visual impairment were twice as likely to have cognitive dysfunction than those with good vision.<sup>S11</sup>

**Supplementary Table 1** summarizes research on the relationship between common eye diseases, including AMD,<sup>S2-S5</sup> DR<sup>S5</sup> and open-angle glaucoma,<sup>S5-S7</sup> with AD dementia. These

epidemiological relationships suggest shared risk factors (e.g., hypertension, smoking) and possibly pathogenic pathways (e.g. neurodegeneration, amyloid- $\beta$  deposits, chronic microvascular insults) between these ocular diseases and AD dementia. However, the associations have not been consistently observed in the literature, particularly in studies at a population-level using large data linkage.<sup>S2,S3,S7</sup> For example, a linkage study using English National Health Service data (AD cohort n=251,703, reference cohort n>2.5M), found no associations between AMD (relative risk: 0.86 [0.67-1.08], compared with the reference cohort) and glaucoma (rate ratio: 1.01 [0.96, 1.06], compared with the reference cohort) with AD dementia.<sup>S2,S7</sup> Lee *et al.* however suggested that the patterns of associations between eye diseases and AD dementia may be different when the ocular conditions are categorized as recent (diagnosed within 0-5 years) or established (>5 years) diagnoses.<sup>S5</sup> They found only established AMD (hazard ratio: 1.50 [1.25, 1.8]) and recent glaucoma (hazard ratio: 1.46 [1.08, 1.91]) are associated with AD dementia, while both established DR (hazard ratio: 1.50 [1.05, 2.15]) and recent DR (hazard ratio: 1.67 [1.01, 2.74]) are associated with AD dementia.<sup>S5</sup> A recent meta-analysis (21 studies, 7,876,499 study subjects) reported that patients with AD dementia are at greater risk for AMD (odds ratio: 2.22,  $I^2=50\%$ ), and patients with AMD are also at increased risk of AD dementia/cognitive dementia (odds ratio:2.42,  $I^2=38\%$ ).<sup>15</sup> Hence, it is likely that AD dementia and common eye diseases are linked via complex, inter-linked, multi-mechanistic pathophysiology and pathways.

### **3. Retinal Imaging Measures and AD**

#### *3.1 Retinal neuronal layer changes at optic disc and macula*

AD is classically characterised by loss of neurons and synapses in the cerebral cortex and specific subcortical regions. Previous histological studies have demonstrated that patients with AD also have loss of retinal ganglion cells (RGCs) and their axons.<sup>S20,S21</sup> A more recent *postmortem* study further suggested that the number of melanopsin RGCs, photoreceptors driving circadian photoentrainment, may be reduced in AD.<sup>14</sup> These observations have been the basis of clinical studies using OCT to determine the relationship between different retinal layers and AD.

The retinal nerve fiber layer (RNFL) surrounding the optic disc (peripapillary RNFL) reflects RGC axons (**Figure 1**). RNFL thickness can be measured by techniques including time-domain OCT (first generation of OCT)<sup>S22-S32</sup> as well as confocal scanning laser ophthalmoscopy<sup>S33</sup> and scanning laser polarimetry.<sup>S34</sup> These studies showed that in AD dementia patients, there is a significant reduction in RNFL thickness compared to age-matched cognitively normal controls.

Spectral-domain OCT (SD-OCT) and swept-source OCT, a newer generation of OCT, provides information on inner retinal layers with greater resolution, such as the ganglion cell layer and the inner-plexiform layer (**Figure 2**).<sup>S35</sup> SD-OCT is now routinely used to not only to measure peripapillary RNFL but also to assess RGC cell body and dendrites together by segmenting and quantifying the thickness of the ganglion cell inner plexiform layer (GC-IPL, a combination of the ganglion cell layer and the inner plexiform layer) at the macula, since this region contains more than 50% of the total RGCs volume.<sup>S36</sup> Numerous studies have investigated the association between SD-OCT measures and AD (**Supplementary Table 2**). These studies first showed that SD-OCT measurements of both peripapillary RNFL (inter-visit intra-class correlation coefficient [ICC]: 0.927 [range: 0.845–0.961] and coefficients of variation [CoV]: 3.83% [range: 2.71–5.25%]), and GC-IPL (inter-visit ICC was 0.968 (0.941–0.985), and CoV was 1.91% [range: 1.24–2.32%]) are reproducible in patients with cognitive impairment.<sup>S37</sup> Second, while a few studies

have reported thicker retinal layers in eyes of patients with AD dementia compared to controls,<sup>S38,S39</sup> or no significant thickness differences,<sup>16,17</sup> the majority of studies, including a meta-analysis, indicate that patients with AD dementia have thinner peripapillary RNFL (standardized mean difference [SMD]= -0.67;  $I^2 = 89\%$ ) and macular GC-IPL (SMD= -0.46,  $I^2 = 71\%$ ) compared with controls,<sup>18</sup> consistent with a human *postmortem* study.<sup>19</sup>

Of the two SD-OCT measurements, some studies suggested that macular GC-IPL may be more sensitive than peripapillary RNFL for assessing neurodegeneration related to AD.<sup>20,21</sup> For example, Cheung et al reported that macular GC-IPL has a better performance to discriminate AD from normal controls than that of peripapillary RNFL (area under receiver operating characteristic curves [AUROCs] 0.685 vs. 0.601), adjusting for age and gender.<sup>20</sup> **Figure 2B and 2C** show an example of GC-IPL and RNFL measurement in a MCI subject with a positive cerebral amyloid PET imaging. Finally, these OCT studies are also consistent with research on other neurodegenerative diseases, such as patients with Parkinson disease and Lewy body dementia, who also have thinner RNFL and thinner inner retinal layers.<sup>S40,S41</sup> Furthermore, thinner RNFL, GC-IPL and ganglion cell layer are also associated with reduced cerebral grey matter and white matter volumes and brain volume measured from MRI.<sup>22-26</sup>

Several possibilities have been proposed to explain the above findings on thinning of the retinal neuronal layer.<sup>18,27</sup> First, the cerebral pathology of AD may affect the neuronal connections of the visual tract and cause retrograde degeneration of the optic nerve and retinal layers, resulting in thinner retinal neuronal and axonal layers including RNFL and GC-IPL.<sup>27</sup> However, peripapillary RNFL could not discriminate controls from AD patients with posterior cortical atrophy, a clinical variant of AD with dominant involvement of parieto-occipital (i.e. visual) cortex, where one would explicitly expect this retrograde degeneration to occur.<sup>S42</sup> Alternatively, it is

speculated that cerebral signs of AD pathology including amyloid- $\beta$  plaques, fibrillar tau and signs of neuroinflammation occur simultaneously both in the brain and the retina, underlining a common pathogenesis linking retinal neuronal and axonal layer changes and AD.<sup>S1 S43-S47</sup> The less common observation of thickened RNFL in AD<sup>S38,S39</sup> may be explained by occurrence of reactive gliosis in inner retina, an inflammatory response, during early stages of AD, which may precede retinal neuronal layer thinning or mask underlying subtle retinal neuronal layer thinning on OCT.<sup>S48</sup>

There are fewer prospective studies on the longitudinal relationship of SD-OCT measures and development of cognitive function deterioration and AD dementia.<sup>27-31</sup> The Rotterdam Study (n=3,289) showed that a thinner peripapillary RNFL is associated with a higher risk of developing dementia (per 1- $\mu$ m decrease hazard ratio: 1.02 [1.01, 1.04]), including AD dementia (per 1- $\mu$ m decrease hazard ratio: 1.02 [1.01, 1.04]), independent of cardiovascular risk factors.<sup>27</sup> In addition, longitudinal data from the UK Biobank (n=32,038) enrolling healthy community dwelling participants also showed that thinner RNFL is a precursor of future decline in cognitive function.<sup>28</sup> Specifically, they found that those in the lowest 2 quintiles of baseline peripapillary RNFL distribution had twice the likelihood of a developing a decline in cognitive function over a 3-year follow-up interval compared with those in the top RNFL quintile.<sup>28</sup> In regard to GC-IPL, data from the Rotterdam Study showed that thinner GC-IPL is only associated with prevalent dementia (per 1- $\mu$ m decrease odds ratio: 1.03 [1.00, 1.09]), but not with incident dementia (per 1- $\mu$ m decrease hazard ratio: 1.02 [0.99, 1.05]) or incident AD dementia (per 1- $\mu$ m decrease hazard ratio: 1.02 [0.99, 1.05]).<sup>27</sup> The Rotterdam study group speculated that there may be a time delay between optic nerve degeneration (reflected by RNFL thinning) and RGC loss (reflected by GC-IPL thinning) as the damage to the optic nerve may cause swelling or gliosis formation of the RGC

axons (i.e. RNFL). Therefore, the neurodegenerative process may manifest itself in the retina initially as thinner peripapillary RNFL, after which thinning of GC-IPL follows.<sup>27</sup>

### *3.2 Retinal arteriolar and venular changes*

There is also substantial evidence indicating a vascular disease component in AD pathophysiology. Clinical and epidemiological studies show that vascular diseases and their risk factors commonly accompanies AD.<sup>32</sup> Vascular risk factors are associated with higher cerebral A $\beta$  burden.<sup>33</sup> Comorbidity of cerebrovascular disease and amyloid- $\beta$  is associated with cognitive decline and neurodegeneration.<sup>34</sup> In particular, microvascular or small vessel disease is now thought to be a major contributor to dementia and cognitive decline.<sup>S49-S52</sup> For example, an autopsy-based neuropathological study showed that a large majority of patients diagnosed with AD without clinical evidence of mixed (vascular) dementia, had microvascular pathology including lacunes, cerebral microbleeds and multiple microinfarcts indicative of small vessel disease.<sup>35</sup>

The retinal circulation of arterioles and venules, measuring 100-300  $\mu$ m in size, are the only optically accessible small blood vessels in the human body. The retinal vasculature can be imaged by either conventional retinal photography (**Figure 1A**) or dye-based fluorescein angiography. However, because dye-based fluorescein angiography is invasive, conventional retinal photography has been the most commonly used retinal imaging technique to capture clinical vascular disease signs, such as those typically seen in patients with diabetes or hypertension (e.g. retinal hemorrhage, cotton wool spots, microaneurysms, arteriovenous nicking, enhanced arteriolar light reflex). In addition to these qualitative signs, computerized algorithms have been developed to measure quantitative changes in the retinal vasculature, for instance the calibre of arterioles and venules.<sup>36-38</sup> Furthermore, geometric patterns of the retinal vasculature may also

provide information on microvascular health. Based on Murray's principle of minimum work, the human circulatory system is a branching system that conforms to optimum design principal to minimize the energy required to maintain blood flow.<sup>S53</sup> Algorithms estimating a number of retinal geometric parameters such as fractal dimension, tortuosity and bifurcation have been further reported.<sup>S54-S61</sup> These algorithms capture deviations from the normal optimal architecture of the retinal vascular network . Several algorithms can be used to analyze retinal photographs taken by conventional retinal cameras. **Figure 1B and 1C** show examples of quantitative retinal vasculature analysis using a widely used software, the Singapore I Vessel Assessment (SIVA), in a cognitively normal subject and a subject with AD, respectively. Other software and algorithms include IVAN (Integrative Vessel Analysis),<sup>36</sup> VAMPIRE (Vascular Assessment and Measurement Platform for Images of the REtina),<sup>S57</sup> and QUARTZ (QUantitative Analysis of Retinal vessel Topology and siZe).<sup>S58</sup>

**Supplementary Table 2** summarizes the clinical studies reporting relationship of quantitative retinal vasculature analysis from retinal photographs with AD. In general, these studies showed a sparser retinal vascular network (indicated by decreased retinal vascular fractal dimension) is associated with AD dementia,<sup>39-42</sup> poorer cognitive test score performances<sup>43,44</sup> and MRI markers of cerebral small vessel disease.<sup>45</sup> For example, Frost et al found that decreased arteriolar fractal dimension (1.201 vs. 1.235,  $p=0.008$ ) and venular fractal dimension (1.171 vs. 1.210,  $p<0.001$ ) in AD dimension, compared with controls.<sup>39</sup> Cheung et al found that decreased arteriolar fractal dimension (per-standard deviation [SD] decrease odds ratio 1.35 [1.08, 1.68]) and venular fractal dimension (per-SD decrease odds ratio 1.47 [1.17, 1.84]) are associated with AD dementia.<sup>40</sup> These findings suggest that changes in the retinal vascular fractal dimension may also reflect a departure from optimal integrity of the cerebral microcirculation (e.g., rarefaction) related

to cognitive impairment.<sup>46</sup> Studies also showed that narrower retinal venular calibre is associated with AD dementia, which may be related to an increased venous wall thickness due to collagen deposition in cerebral veins.<sup>39,40</sup> Although some studies observed significant associations between retinal vascular tortuosity and AD dementia, the relationship remains equivocal. Cheung *et al.*<sup>40</sup> found that both increased retinal arteriolar (per-SD increase odds ratio 1.80 [1.40, 2.31]) and venular tortuosity (per-SD increase odds ratio 1.94 [1.48, 2.53]) are associated with AD dementia, while Williams *et al.*<sup>41</sup> found that decreased retinal arteriolar (per-SD increase OR 0.78 [0.63, 0.97]) tortuosity is associated with AD dementia. It is noted that increased retinal vascular tortuosity is associated with higher blood pressure and diabetes,<sup>S59,S62</sup> and difference between studies may reflect differences in prevalence of hypertension and diabetes (e.g. participants in the study by Cheung *et al* had higher prevalence of both hypertension and diabetes than participants in studies by Williams and Frost). On the other hand, if different pathophysiological mechanisms occur at different stages of AD,<sup>47</sup> associations with retinal parameters would be expected to change correspondingly. Thus, clinical and demographic data and stages of AD should be taken into account when interpreting findings across studies.

### *3.3 Retinal capillary changes*

In addition to the arterioles and venules, changes at the capillary level (5 to 15  $\mu\text{m}$ ) may also be studied for their relationship to AD.<sup>48,49</sup> The retinal capillary network can now be imaged by dye-free OCT-angiography (OCT-A) which visualizes capillary levels at different levels and sites of the retina: the superficial capillary plexus, the deep capillary plexus and the radial peripapillary capillary plexus. Images captured by OCT-A (**Figure 3**) have helped to identify and quantify capillary level abnormalities in primary retinal diseases such as DR and AMD.<sup>S63-S66</sup>

**Supplementary Figure 1** shows image processing steps adopted to quantify the capillary networks from OCT-A images.<sup>S63</sup> Recent reports (**Supplementary Table 2**) have identified changes in the retinal capillary networks using OCT-A in AD dementia and preclinical AD.<sup>S67-S75</sup> For example, Bulut *et al.* observed decreased capillary network density (45.5% vs. 48.7%,  $p=0.002$ ) and an enlarged foveal avascular zone area ( $0.47\text{mm}^2$  vs.  $0.33\text{mm}^2$ ,  $p=0.001$ ) in 26 patients with AD dementia, compared with 26 age- and sex-match controls.<sup>S67</sup> O'Bryhim *et al.* further demonstrated that enlarged foveal avascular zone measured from OCT-A is associated with preclinical AD ( $0.364\text{mm}^2$  vs.  $0.275\text{mm}^2$ ,  $p=0.002$ ), as defined by presence of amyloid- $\beta$  biomarkers from PET or CSF, compared with those amyloid- $\beta$ -negative control subjects ( $n=32$  participants).<sup>S74</sup> In addition, they reported that foveal avascular zone area can discriminate participants with biomarker-positive and biomarker-negative with an AUROC of 0.801.<sup>S74</sup> These observations are in line with disturbances in the morphology and function of cerebral capillary networks observed as antecedents to neurodegenerative changes associated with AD in animal models and *postmortem* studies.<sup>S76-S78</sup> However, the current literature is not entirely consistent. For example, Querques *et al.* and den Haan *et al.* did not observe any differences in capillary network density and foveal avascular zone between patients with AD dementia and controls.<sup>S71,S72</sup> Van de Kreeke *et al.* have reported that an increased capillary network density in patients with preclinical AD, instead of a decreased one, compared with controls (inner ring macula difference: 0.81%,  $p=0.002$ ; outer ring macula difference: 0.50%,  $p=0.024$ ; and around optic nerve head difference: 0.83%,  $p=0.015$ ), which may be due to an inflammatory state of the retina in the early stages of amyloid- $\beta$  accumulation.<sup>S75</sup> It is noteworthy that similar to the literature on retinal imaging technologies as mentioned above, the diagnosis of AD dementia differ between different

OCT-A studies, and most of studies are currently limited by small sample size and the inability to adequately account for potential confounding factors (e.g. diabetes, axial length of the eyeball).

### *3.4 Choroidal vasculature changes*

Deep to the retina, the choroid contributes blood supply to the outer retina. In addition to the retinal vasculature (arterioles, venules, capillary network), SD-OCT with enhanced depth imaging, or swept-source OCT, has now made it possible to image the choroidal vasculature. **Figure 2D and 2E** show a cross-sectional view of the choroidal vasculature imaged by SS-OCT in a cognitively normal subject and a subject with AD, respectively. A few case-control studies have observed thinning of the choroidal layer as assessed by SD-OCT with enhanced depth imaging in AD dementia (**Supplementary Table 2**).<sup>S67,S79,S80</sup> For example, Gharbiya et al. firstly reported reduced subfoveal choroidal thicknesses (200.9 $\mu$ m vs. 266.1 $\mu$ m,  $p=0.001$ ) in 21 patients with mild to moderate AD dementia, compared with controls. It was postulated that choroidal thinning indicates an abnormal choroidal blood supply associated with vasoregression or atrophic changes related to a series of pathologic events (e.g. inflammatory cascade) triggered by amyloid- $\beta$  deposition in the brain.<sup>S80,S81</sup> In a recent prospective study ( $n=78$ ), a larger reduction in choroidal thicknesses is observed in AD dementia over a 12-month follow-up (changes in subfoveal choroidal thickness: -10.47 $\mu$ m vs. -2.0  $\mu$ m), compared with controls.<sup>S81</sup> This finding is consistent with a report on *postmortem* eyes from AD dementia patients and animal models of AD.<sup>S82</sup> Furthermore, a population-based study with more than 3,000 participants found reduced subfoveal choroidal thickness is significantly associated with lower Mini Mental Status Examination score, in line with the findings in AD dementia eyes.<sup>S83</sup>

### 3.5 Vasodilatory response changes

The retinal NVU contains neurons, glial cells and vascular cells, similar to the NVU in the CNS.<sup>13</sup> Flickering light stimulates activity of the neural retina and leads to retinal vessel dilation as a result of the release of vasodilating factors, especially nitric oxide, from endothelial and neural cells. This dynamic reaction of retinal vessels to flickering light is influenced by neurovascular coupling and can therefore be used to assess the function of NVU in the retina.<sup>S84</sup> The flicker-induced vasodilatory response can now be measured non-invasively using a dynamic vessel analyser (DVA). A few studies have explored to use DVA to investigate the flicker-induced vasodilatory response in AD, but the current findings are still preliminary and inconclusive. Kotliar *et al.* observed that overall flicker-induced vasodilatory response is delayed in AD dementia (arterial time to reach 30% of maximum dilation: 7.0 seconds vs. 5.0 seconds,  $p < 0.001$ ), compared with controls, suggesting delayed arterial reaction in AD.<sup>50</sup> They also demonstrated that this DVA parameter can discriminate AD dementia with an AUROC of 0.853.<sup>50</sup> However, Golzan *et al.* only found a positive correlation between neocortical amyloid- $\beta$  standardised uptake value ratio (SUVR) measured by PET with the amplitude of retinal arterial pulsations, but did not observe any correlations with dynamic flicker-induced retinal arteriolar or venular dilation in an elderly cohort.<sup>51</sup> It is noteworthy that patients with diabetes and DR have reduced flicker-induced vasodilatory response.<sup>S85,S86</sup> Kotliar's and Golzan's studies did not specifically exclude those with diabetes and with ocular diseases, which may confound the results reported. Querques *et al.* recently conducted a similar study but excluded subjects with diabetes and optic nerve or retinal diseases and reported that retinal arteriolar dilation in response to flickering light is reduced in the AD dementia group, compared with controls (0.77% vs. 3.53%,  $p = 0.002$ ) and the MCI group (0.77% vs. 2.84%,  $p = 0.045$ ).<sup>S71</sup> This study suggests that the neurovascular coupling of retinal vessels in

AD dementia is impaired, especially in retinal arterioles, and the effect is independent of diabetes. This observation suggests that decreased retinal and cerebral blood flow (i.e. hypoperfusion) might impair the endothelial function and the production of nitric oxide, which is vital for the vasodilatation process.<sup>52, S71</sup>

### *3.6 Retinal vessel oxygen saturation changes*

The retina is one of the most metabolically active tissues in the human body. Retinal vessel oxygen saturation can now also be measured noninvasively, based on estimation of haemoglobin oxygen saturation in retinal vessels by taking two simultaneous retinal photographs with 570- and 600-nm light.<sup>S87</sup> Studies have reported that retinal oxygen saturation in arterioles and venules is significantly higher in both AD dementia and MCI eyes, compared with controls.<sup>S88, S89</sup> Einarsdottir et al showed that retinal arterioles have  $94.2 \pm 5.4\%$  oxygen saturation in moderate AD compared with  $90.5 \pm 3.1\%$  in healthy subjects ( $p=0.028$ ). Retinal venules were  $51.9 \pm 6.0\%$  saturated in moderate AD compared with  $49.7 \pm 7.0\%$  in healthy subjects ( $p=0.02$ ).<sup>S88</sup> Olafsdottir et al further showed that arteriolar and venular oxygen saturation was increased in MCI patients, compared with healthy individuals ( $93.1 \pm 3.7\%$  vs.  $91.1 \pm 3.4\%$ ,  $p=0.01$ ;  $59.6 \pm 6.1\%$  vs.  $54.9 \pm 6.4\%$ ,  $p=0.001$ , respectively).<sup>S89</sup> These studies demonstrate a decreased metabolic activity in the retina and this exploratory finding may provide new insight into the pathophysiology of AD related to hypometabolism.

### *3.7 Peripheral retinal changes*

Drusen deposits are the hallmark of AMD. Amyloid- $\beta$  has been found in drusen deposits in the retina.<sup>S90</sup> In a recent pilot study, Csincsik *et al.* utilized ultra-widefield scanning laser

ophthalmoscopy and examined AMD-like drusen deposits in a wider field of the peripheral retina, in addition to the macular region.<sup>42</sup> They found that patients with AD dementia are more likely to have drusen deposits in the peripheral retina compared to controls (25.4% vs. 4.2%,  $p=0.04$ ), especially in the superior nasal quadrant.<sup>42</sup> **Supplementary Figure 2** shows an example of presence of drusen deposits in the peripheral retina imaged by ultra-widefield scanning laser ophthalmoscopy in a subject with AD dementia. In addition, Ukalovin *et al.* also found that the severity of cerebral amyloid angiopathy, a vascular feature associated with AD dementia and cognitive decline,<sup>S91</sup> is correlated with the number of drusen in the peripheral retina from *postmortem* AD eyes ( $r=0.78$ ,  $p<0.05$ ).<sup>S92</sup> The preliminary findings from these exploratory studies suggest that retinal abnormalities related to AD are also present in peripheral retina, in addition to retinal changes measured from conventional retinal imaging areas focused centrally (i.e. macular and optic disc regions). Further studies are required to determine whether the peripheral retinal changes have similar or additional predictive value for AD dementia or cognitive decline, and to develop better understanding of the significance of these associations, particularly since peripheral changes can also occur in the intermediate to advanced stage of AMD.<sup>S93</sup>

### 3.8 Retinal fluorescence lifetime changes

The retina has several kinds of endogenous fluorophores, including lipofuscin, advanced glycation end products, collagen, melanin, and elastin. Retinal fluorophores can be excited by monochromatic light (e.g. laser) and gain a higher level of energy before returning to their ground state by emitting photons of longer wavelengths than the exciting light (i.e. fluorescence lifetime).<sup>S94</sup> Each fluorophore possesses a characteristic fluorescence lifetime. Fluorescence lifetime imaging ophthalmoscopy (FLIO) is a technique for measuring fluorescence lifetime,

which is calculated by the average amount of time a fluorophore remains in the excited state following excitation, to allow detecting metabolic alterations in the retina for various retinal disease such as AMD at an early stage.<sup>S94</sup> Jentsch *et al.* found that a longer retinal fluorescence lifetime measured by FLIO is correlated with higher tau protein concentration in CSF in patients with AD dementia.<sup>S95</sup> In a pilot study, Sadda *et al.* also found that subjects with preclinical AD, compared with controls, have longer retinal fluorescence lifetime ( $593.9 \pm 93.3$ ,  $454.4 \pm 38.6$  picosecond;  $475.0 \pm 71.6$ ,  $394.1 \pm 28.2$  picosecond in short spectral channel and long spectral channel of AD and control groups, respectively,  $p = 0.036$  and  $0.024$ ), which is also correlated with GC-IPL thickness, amyloid- $\beta$  and tau protein in CSF.<sup>S96</sup> The preliminary findings from these exploratory studies suggest that the fluorophore composition in the retina may be related to AD.

#### **4. Age-related effect on the retina**

Age-related changes are well-reported in the retinal neuronal and vascular structures as well as in the choroid. RNFL and GC-IPL thicknesses decrease with increasing age in healthy adults.<sup>S97-S99</sup> In a longitudinal analysis, the mean rate of change of average RNFL is  $-0.52\mu\text{m}/\text{year}$  in normal individuals.<sup>S100</sup> Similarly, narrower retinal vessel caliber, straighter retinal vessels, sparser retinal vasculature and decreased choroidal thickness are correlated with increasing age in healthy adults as reported from population-based studies.<sup>S101-S105</sup> In the Singapore Malay Eye Study-2, for each 1-year increase in age, subfoveal choroidal thickness decreased by  $3.10\mu\text{m}$ .<sup>S104</sup> These age-related effect on retinal imaging measures are considered as a physiological process; however, the current measurements are not standardized by age. Although most of the reported studies were case-control study design matched with age or included age as a confounding factor in the statistical

models, how to taking aging effect into account during image interpretation in clinical practice should be further addressed.

## **5. Evidence of AD pathology in the retina is equivocal**

Amyloid- $\beta$  protein plaques and neurofibrillary tangles comprised of hyperphosphorylated tau protein are pathological hallmarks of AD. Several histopathological studies have identified retinal amyloid- $\beta$  deposits in animal models of AD<sup>S82,S106</sup> as well as human subjects with definite AD<sup>14,S1</sup> and suspected early AD.<sup>S44</sup> The majority of amyloid- $\beta$  deposits are in the GC-IPL,<sup>S46</sup> and some show perivascular clustering.<sup>14, S1</sup> A clinical study by Koronyo *et al.* also demonstrated an increased presence of amyloid- $\beta$  in the retina of AD dementia patients compared to controls, especially in the peripheral superior quadrant, often clustered along blood vessels.<sup>S1</sup> These retinal amyloid- $\beta$  plaques qualitatively resemble those found in the cerebrum of AD dementia subjects and were only detected in minimal quantities in age-matched non-AD controls.<sup>14, S1</sup> Moreover, it is possible that accumulation of retinal amyloid- $\beta$  plaques occurs earlier than in the brain and the amount increases with disease progression.<sup>S44</sup> Similar to those in the brain, retinal amyloid- $\beta$  deposition also showed to be associated with marked neurodegeneration. La Morgia *et al.* demonstrated that there is amyloid- $\beta$  deposition in and around degenerating melanopsin RGCs, suggesting amyloid- $\beta$  is toxic to retinal neurons.<sup>14</sup> Koronyo *et al.* also reported that, when compared to matched controls, reduced cell counts in the RGC layer, inner nuclear layer and outer nuclear layer are observed in AD dementia patients along with accumulation of amyloid- $\beta$ .<sup>S1</sup> In line with these findings, the neurotoxicity of amyloid- $\beta$  to retinal neurons has also been shown in both cell-line studies<sup>S107,S108</sup> and animal model studies.<sup>S43,S109,S110</sup> These findings from animal studies are therefore consistent with the observations of clinical studies reporting thinner RNFL

and GC-IPL in patients with AD dementia discussed above. Apart from retinal amyloid- $\beta$  deposition, animal studies also showed that there are tau aggregates in the retina of transgenic mice with a tau mutation.<sup>S111</sup> These mice display abnormal neurotrophic factor signaling, increased susceptibility to excitotoxic damage, early axonopathy, and functional deficits of RGCs.<sup>S111,S112</sup>

However, it is noteworthy that the evidence of AD pathology in the retina is not consistent across the literature, and presence of amyloid- $\beta$  or tau in the retina still remains controversial.<sup>S113</sup> For example, Schön *et al.* reported that the *postmortem* retinas of AD dementia patients only contain hyperphosphorylated tau but not amyloid- $\beta$  or fibrillar tau aggregates.<sup>S45</sup> Several studies did not find any AD related pathology in AD retinas, and could not replicate previous findings.<sup>S21,S114,S115</sup> Haan *et al.* found that despite amyloid- $\beta$ /amyloid precursor protein being present in *postmortem* AD retinas, there are no amyloid- $\beta$ /amyloid precursor protein related differences, but rather tau related changes, between AD and control retinas.<sup>S116</sup> It is noted that adoption of different tissue processing methods and immunostaining protocols, and co-morbidity of ocular diseases and AD may possibly explain some discrepancies. On the other hand, although amyloid is proclaimed as a toxic substance, it triggers the pathological process in the very initial state of the disease. For instance, hippocampal volume is characteristically reduced in AD with congruent tau pathology in the corresponding region, whereas it lacks amyloid pathology in hippocampal region.<sup>S117</sup> Findings on presence of amyloid- $\beta$  or tau in the retina should be further replicated before we assume that AD pathology in the retina is present. Furthermore, studies on relationships among amyloid, tau and retinal changes in the pathological study of AD are warranted.

## 6. Future Research

Studies to date suggest a range of retinal imaging technologies can be utilized to study different stages of AD. However, more research is clearly needed. For example, studies on relationships between retinal imaging measures and "standard" biomarkers of AD pathophysiology, as well as direct comparisons between different retinal imaging measures to determine relative sensitivity/specificity of each measure for AD clinical diagnosis or biomarker status are warranted. Furthermore, some neuronal and vascular changes in the retina are similar between AD and ocular disease. Some of these researches are discussed below.

### *6.1 Framework of Development and Validation of Retinal Imaging as a Source of Biomarkers*

Disease-modifying treatments for AD are most likely to be successful if initiated early in the disease process, ideally before irreversible neurodegeneration and functional decline set in.<sup>53,54</sup> Biomarkers may aid in risk profiling to identify those at greatest risk, detection of pathology at the earliest possible stage, and by providing end points for trials that identify benefit earlier in the natural history of the disease, thus accelerating the development of new treatments. Therefore, discovering effective biomarkers of AD is a priority for development of new treatment.

A biomarker is defined as an objective substance, characteristic, or other parameter of a biological process that enables the assessment of a disease risk or prognosis and provides guidance for diagnosis or monitoring of treatment.<sup>10</sup> Different groups have proposed frameworks or roadmaps for biomarker development and validation for AD.<sup>9, 10, 55,56</sup> For example, Frisoni *et al.* proposed a five-phase framework to foster the clinical validation of biomarkers for an early diagnosis of AD, adapted from the approach for cancer biomarkers. These include preclinical exploratory studies, clinical assay development for AD pathology, retrospective studies using longitudinal data available in repositories, prospective diagnostic accuracy studies, and disease

burden reduction studies.<sup>10</sup> A consistent framework to assess the validity of biomarkers for different clinical purposes is essentially important for implementation and clinical use in AD.

Currently, retinal imaging technologies cannot yet be considered a source of biomarker of AD as many areas of research remain conflicting and evidence-based guidelines on the use and interpretation of retinal imaging are currently lacking. Most published studies have focused on demonstrating measure difference compared with controls and associations (linear or logistic regression models) between a set of retinal imaging measures with AD dementia only. Moreover, studies on preclinical AD are largely lacking. **Table 2** summarizes the findings on retinal neuronal changes, retinal capillary changes, retinal arteriolar and venular changes, and choroidal vasculature changes. In addition, some of the reported associations may not account for potential confounding factors (e.g. ocular diseases and systemic conditions) and clinical stages of AD. The current retinal imaging features (e.g., RNFL loss) are also non-specific to AD and not designed to fully describe and characterize the spectrum of AD-related disorders. For example, there is a lack of consensus on how best to differentiate between retinal changes seen in glaucoma and AD dementia. Typically, in patients with glaucoma, the reduction in peripapillary RNFL occurs in inferior and superior sectors<sup>S118</sup> but the studies in AD dementia have also shown similar patterns of RNFL reduction.<sup>18</sup> Many prior studies have also not evaluated retinal imaging for a specific clinical purpose such as screening, diagnosis, prognosis or monitoring of AD dementia. Appropriate statistical analysis of biomarker validation should be performed (e.g. performing area under the receiver operating characteristic curve to evaluate discriminative performance). Finally, the definition of AD in the reports did not consistently include confirmation from current available biomarkers. Thus, there is inadequate evidence on the clinical usefulness of retinal imaging measures as a biomarker for AD.

We suggest the following framework of research (**Supplementary Table 3**). First, studies should be designed and conducted to validate biomarkers from retinal images with a specific clinical purpose (e.g. screening or risk stratification). Second, diagnosis of AD should be defined in a consistent manner with the latest available criteria (e.g. confirmation with current biomarkers). Third, standard statistical measures of accuracy of biomarkers should be reported. For example, if a study evaluates measures from retinal images as a potential screening tool, the sensitivity, specificity, false-positive and false-negative rates of retinal imaging should be reported. The degree of abnormality and the prevalence (i.e. how frequent is the abnormality found in AD) should be described. Fourth, studies should be designed carefully to take into account many age-related ocular conditions. The effects of ocular factors (e.g. axial length of the eyeball) on retinal imaging measures and the associations with common eye diseases (e.g. glaucoma and AMD) should be determined and considered in the analysis and interpretation. Fifth, the reproducibility of the retinal imaging measures should be determined, particularly if retinal imaging is used for disease diagnosis and monitoring on multiple follow-up visits. Finally, the incremental benefit and cost-effectiveness of retinal imaging as well as acceptability to patients in different settings should be evaluated. These areas should be reported in the framework of retinal imaging studies for AD.

## *6.2 Other New Retinal Imaging Technologies Related to AD*

Several new retinal imaging technologies are also being explored which might provide additional value in this field.

Retinal hyperspectral imaging obtains a series of hyperspectral reflectance images, combining both spectral and spatial information, by scanning the retina with a continuous range of wavelengths of light.<sup>S119</sup> More *et al* showed that amyloid- $\beta$  exerts a characteristic influence on the

reflectance of light as assessed by retinal hyperspectral imaging and that the magnitude of this effect varies in proportion with the amount of amyloid- $\beta$  in the retina of AD mouse.<sup>S120,S121</sup> This finding was further validated in recent *in vivo* human clinical studies by showing optical density spectral profiles are different between AD and controls,<sup>S122</sup> and cases who are amyloid- $\beta$  positive and negative on PET can be discriminated from the reflectance of hyperspectral retinal images with a machine learning based model for the classification.<sup>S123,S124</sup> Hyperspectral imaging technology is also being investigated to identify brain cancer<sup>S125</sup> as well as to estimate cerebral metabolism and hemodynamics from brain tissues.<sup>S126</sup>

Adaptive optics , improving the performance of optical systems by reducing the effects of optical aberrations, can be employed in scanning laser ophthalmoscopy to achieve very high resolution ( $\sim 2\mu\text{m}$ ) in the human retina resulting in the direct visualization of nerve fibre bundles and other minute retinal features.<sup>S127</sup> Zhang *et al.* found that individuals with MCI have a significantly higher number of hyperreflective granular membranes at the peripapillary area covered the RNFL as assessed by adaptive optics scanning laser ophthalmoscopy.<sup>S48</sup> The authors speculated that the hyperreflective granular membranes are due to inner retinal gliosis which supports a previously established association between AD and glial cell activation in the brain and retina.<sup>S128,S129</sup>

Given that the retina is an easily accessible window and connected to the CNS, it is believed that further advance in retinal imaging as well as multi-modal, composite biomarkers for AD will be continuously developed.

### 6.3. Artificial intelligence

Another major area of future research in the analysis of retinal images is AI. The current retinal imaging measures (e.g. reduction in RNFL thickness) are not necessarily specific to AD and not designed to fully describe and characterize the spectrum of AD-related disorders. Recent developments of AI, particularly in DL, have potential to transform imaging technology in healthcare.<sup>S130,S131</sup> DL is based on deep neural networks, involving many layers of linear (convolutional) and nonlinear operations trained on previously unfeasible amounts of data.

In retinal imaging, AI and DL technology have been developed in several areas, the two most prominent ones being first, in the assessment of retinal photographs for detection and screening of DR,<sup>S132-S137</sup> AMD,<sup>S138-S140</sup> glaucoma,<sup>S141, S142</sup> and retinopathy of prematurity,<sup>S143,S144</sup> and second, the segmentation and assessment of OCT images for diagnosis and screening of major retinal diseases.<sup>S145-S148</sup> These studies demonstrate the promise of DL for discovering discriminative latent information associated with AD as well as neurodegenerative disease and cerebrovascular disease from retinal images.<sup>S149,S150</sup> For example, using DL, target-specific features are automatically learnt by DL algorithm in the feature extraction stage and numerous unconventional features that are neither noticed by human previously nor examined by appropriate clinical study will also be assessed. DL could be used to recognize specific pattern of retinal changes secondary to AD pathology (i.e. “retinal fingerprint” of AD) potentially.

How might AI based retinal imaging be used potentially? **Supplementary Figure 3** shows a proposed pathway of screening AD using retinal imaging. By providing a simple 2-tier risk stratification output, this algorithm could assist physicians to identify asymptomatic individuals who are more likely to have AD in the community. The availability of retinal imaging in eye clinics for assessing ocular diseases allows opportunistic screening for AD on a large scale. Introducing retinal imaging in neurology clinics for subjects with memory issues would add a complementary

risk profiling tool for assessing the risk of AD. Higher-risk patients could then benefit from subsequent more intensive and specific (but expensive) examinations (e.g. PET imaging of CSF analysis for identification of underlying disease pathologies). This would potentially benefit the treatment workflow of AD if a disease-modifying therapy is successfully developed.

#### *6.4 Clinical trials and outcome monitoring*

While retinal imaging cannot fully replace current tests such as PET imaging or CSF analysis for detecting AD pathology (e.g. amyloid- $\beta$  and tau accumulation), retinal imaging offers several unique advantages over current biomarkers. First, retinal imaging offers lower costs methods to identify appropriate study cohorts (i.e. cognitively normal individuals with AD-related retinal characteristics) for recruitment into clinical trials of new treatments for dementia (e.g. anti-amyloid therapy to delay cognitive decline). Measurements from retinal imaging (e.g. neuronal and vascular changes) may also be used to assess optimal or suboptimal therapeutic response to medical intervention. For example, the ENVIS-ion study, which aims to determine the effectiveness of low-dose aspirin in reducing the development of white-matter lesion and silent brain infraction, is also validating retinal vascular changes as potential treatment outcomes.<sup>57</sup> In addition, blood-based biomarkers, a less invasive and potentially cheaper approach, are being explored for aiding AD detection at early stage.<sup>58,59,S151-S152</sup> Combining both retinal imaging and blood-based biomarkers (i.e. “multiple marker approach”) may increase the accuracy to identify appropriate study cohorts for recruitment into the clinical trials, compared with using only a single marker.

## **7. Conclusions**

There is an increasing body of research using current and emerging retinal imaging technology to study AD. Newer retinal imaging technologies are increasingly available, are non-invasive, and comparatively low cost and easy to use for clinical and population studies. While current research shows promising evidence that many retinal imaging measures show associations with AD, longitudinal studies are lacking and larger replication studies are necessary. A framework for retinal imaging development and validation in AD should be developed, and followed by future studies to allow consistent comparison of findings. Newer computational technology, such as AI hold promise to use retinal imaging as a “point of care” level test for screening, early risk assessment and stratification.

**Contributorship** TYW, CC and CYC conceptualized and designed the article. CYC drafted the article. CYC, VM, PJF, ET, CC and TYW were responsible for revising it critically for important intellectual content. All authors approved this version to be published.

### **Funding statement**

CYC has received grant funding from the Health and Medical Research Fund, Hong Kong (Grant Number: 04153506) and Bright Focus Foundation (Reference Number: A2018093S).

VM has received grant funding from SEEDS Foundation Ltd.

PF has received grant support for this work from The Richard Desmond Charitable Foundation via Fight for Sight, London, UK (Grant code 1965), The International Glaucoma Association, Ashford, UK and The Alcon Research Institute, Fort Worth, Texas, USA.

CC has received grant funding from the National Medical Research Council Singapore (NMRC/CG/NUHS/2010 and NMRC/CG/013/2013).

ET has received grant funding from the EPSRC (M005976/1) and the NIHR Global Health Research Unit “INSPIRED” (16/136/102).

TYW has received grant funding from the National Medical Research Council Singapore (NMRC/STaR/016/2013 and NMRC/OFLCG/001c/2017) and Duke-NUS Medical School (DUKE-NUS/RSF/2014/0001).

There is no role of the funding sources.

### **Competing of Interests**

None

### **Acknowledgments**

We would like to acknowledge Dr Victor Chan from the Chinese University of Hong Kong, Hong Kong, China; Dr Saima Hilal from National University of Singapore, Singapore; Dr Narayanaswamy Venketasubramanian from the Raffles Hospital, Singapore; and Dr M. Kamran Ikram from Erasmus Medical Center, The Netherlands.

## REFERENCES

1. Alzheimer's A. 2016 Alzheimer's disease facts and figures. *Alzheimers Dement* 2016;12(4):459-509.
2. Jack CR, Jr., Knopman DS, Jagust WJ, et al. Tracking pathophysiological processes in Alzheimer's disease: an updated hypothetical model of dynamic biomarkers. *Lancet Neurol* 2013;12(2):207-16. doi: 10.1016/S1474-4422(12)70291-0
3. Sperling R, Mormino E, Johnson K. The evolution of preclinical Alzheimer's disease: implications for prevention trials. *Neuron* 2014;84(3):608-22. doi: 10.1016/j.neuron.2014.10.038
4. Cummings J, Passmore P, McGuinness B, et al. Souvenaid in the management of mild cognitive impairment: an expert consensus opinion. *Alzheimers Res Ther* 2019;11(1):73. doi: 10.1186/s13195-019-0528-6
5. Dubois B, Padovani A, Scheltens P, et al. Timely Diagnosis for Alzheimer's Disease: A Literature Review on Benefits and Challenges. *J Alzheimers Dis* 2016;49(3):617-31. doi: 10.3233/JAD-150692
6. Albert MS, DeKosky ST, Dickson D, et al. The diagnosis of mild cognitive impairment due to Alzheimer's disease: recommendations from the National Institute on Aging-Alzheimer's Association workgroups on diagnostic guidelines for Alzheimer's disease. *Alzheimers Dement* 2011;7(3):270-9. doi: 10.1016/j.jalz.2011.03.008
7. Siemers ER, Sundell KL, Carlson C, et al. Phase 3 solanezumab trials: Secondary outcomes in mild Alzheimer's disease patients. *Alzheimers Dement* 2016;12(2):110-20. doi: 10.1016/j.jalz.2015.06.1893
8. Beach TG, Monsell SE, Phillips LE, et al. Accuracy of the clinical diagnosis of Alzheimer disease at National Institute on Aging Alzheimer Disease Centers, 2005-2010. *J Neuropathol Exp Neurol* 2012;71(4):266-73. doi: 10.1097/NEN.0b013e31824b211b
9. Jack CR, Jr., Bennett DA, Blennow K, et al. NIA-AA Research Framework: Toward a biological definition of Alzheimer's disease. *Alzheimers Dement* 2018;14(4):535-62. doi: 10.1016/j.jalz.2018.02.018
10. Frisoni GB, Boccardi M, Barkhof F, et al. Strategic roadmap for an early diagnosis of Alzheimer's disease based on biomarkers. *Lancet Neurol* 2017;16(8):661-76. doi: 10.1016/S1474-4422(17)30159-X
11. McKhann GM, Knopman DS, Chertkow H, et al. The diagnosis of dementia due to Alzheimer's disease: recommendations from the National Institute on Aging-Alzheimer's

- Association workgroups on diagnostic guidelines for Alzheimer's disease. *AlzheimersDement* 2011;7(3):263-69.
12. London A, Benhar I, Schwartz M. The retina as a window to the brain-from eye research to CNS disorders. *Nat Rev Neurol* 2013;9(1):44-53. doi: 10.1038/nrneuro.2012.227
  13. Antonetti DA, Klein R, Gardner TW. Diabetic retinopathy. *NEnglJ Med* 2012;366(13):1227-39.
  14. La Morgia C, Ross-Cisneros FN, Koronyo Y, et al. Melanopsin retinal ganglion cell loss in Alzheimer disease. *Ann Neurol* 2016;79(1):90-109. doi: 10.1002/ana.24548
  15. Rong SS, Lee BY, Kuk AK, et al. Comorbidity of dementia and age-related macular degeneration calls for clinical awareness: a meta-analysis. *Br J Ophthalmol* 2019;103(12):1777-83. doi: 10.1136/bjophthalmol-2018-313277
  16. Haan JD, van de Kreeke JA, Konijnenberg E, et al. Retinal thickness as a potential biomarker in patients with amyloid-proven early- and late-onset Alzheimer's disease. *Alzheimers Dement (Amst)* 2019;11:463-71. doi: 10.1016/j.dadm.2019.05.002
  17. Sanchez D, Castilla-Marti M, Rodriguez-Gomez O, et al. Usefulness of peripapillary nerve fiber layer thickness assessed by optical coherence tomography as a biomarker for Alzheimer's disease. *Sci Rep* 2018;8(1):16345. doi: 10.1038/s41598-018-34577-3
  18. Chan VTT, Sun Z, Tang S, et al. Spectral-Domain OCT Measurements in Alzheimer's Disease: A Systematic Review and Meta-analysis. *Ophthalmology* 2019;126(4):497-510. doi: 10.1016/j.opthta.2018.08.009
  19. Asanad S, Ross-Cisneros FN, Nassisi M, et al. The Retina in Alzheimer's Disease: Histomorphometric Analysis of an Ophthalmologic Biomarker. *Invest Ophthalmol Vis Sci* 2019;60(5):1491-500. doi: 10.1167/iovs.18-25966
  20. Cheung CY, Ong YT, Hilal S, et al. Retinal ganglion cell analysis using high-definition optical coherence tomography in patients with mild cognitive impairment and Alzheimer's disease. *J Alzheimers Dis* 2015;45(1):45-56. doi: 10.3233/JAD-141659
  21. Ito Y, Sasaki M, Takahashi H, et al. Quantitative Assessment of the Retina Using OCT and Associations with Cognitive Function. *Ophthalmology* 2020;127(1):107-18. doi: 10.1016/j.opthta.2019.05.021
  22. Ong YT, Hilal S, Cheung CY, et al. Retinal neurodegeneration on optical coherence tomography and cerebral atrophy. *Neurosci Lett* 2015;584:12-6. doi: 10.1016/j.neulet.2014.10.010

23. Casaletto KB, Ward ME, Baker NS, et al. Retinal thinning is uniquely associated with medial temporal lobe atrophy in neurologically normal older adults. *Neurobiol Aging* 2017;51:141-47. doi: 10.1016/j.neurobiolaging.2016.12.011
24. Mutlu U, Bonnemaier PWM, Ikram MA, et al. Retinal neurodegeneration and brain MRI markers: the Rotterdam Study. *Neurobiol Aging* 2017;60:183-91. doi: 10.1016/j.neurobiolaging.2017.09.003
25. Mutlu U, Ikram MK, Roshchupkin GV, et al. Thinner retinal layers are associated with changes in the visual pathway: A population-based study. *Hum Brain Mapp* 2018;39(11):4290-301. doi: 10.1002/hbm.24246
26. Tao R, Lu Z, Ding D, et al. Perifovea retinal thickness as an ophthalmic biomarker for mild cognitive impairment and early Alzheimer's disease. *Alzheimers Dement (Amst)* 2019;11:405-14. doi: 10.1016/j.dadm.2019.04.003
27. Mutlu U, Colijn JM, Ikram MA, et al. Association of Retinal Neurodegeneration on Optical Coherence Tomography With Dementia: A Population-Based Study. *JAMA Neurol* 2018;75(10):1256-63. doi: 10.1001/jamaneurol.2018.1563
28. Ko F, Muthy ZA, Gallacher J, et al. Association of Retinal Nerve Fiber Layer Thinning With Current and Future Cognitive Decline: A Study Using Optical Coherence Tomography. *JAMA Neurol* 2018;75(10):1198-205. doi: 10.1001/jamaneurol.2018.1578
29. Shi Z, Wu Y, Wang M, et al. Greater attenuation of retinal nerve fiber layer thickness in Alzheimer's disease patients. *J Alzheimers Dis* 2014;40(2):277-83. doi: 10.3233/JAD-131898
30. Choi SH, Park SJ, Kim NR. Macular Ganglion Cell -Inner Plexiform Layer Thickness Is Associated with Clinical Progression in Mild Cognitive Impairment and Alzheimers Disease. *PLoS One* 2016;11(9):e0162202. doi: 10.1371/journal.pone.0162202
31. Trebbastoni A, D'Antonio F, Bruscolini A, et al. Retinal nerve fibre layer thickness changes in Alzheimer's disease: Results from a 12-month prospective case series. *Neurosci Lett* 2016;629:165-70. doi: 10.1016/j.neulet.2016.07.006
32. Sweeney MD, Montagne A, Sagare AP, et al. Vascular dysfunction-The disregarded partner of Alzheimer's disease. *Alzheimers Dement* 2019;15(1):158-67. doi: 10.1016/j.jalz.2018.07.222
33. Gottesman RF, Schneider AL, Zhou Y, et al. Association Between Midlife Vascular Risk Factors and Estimated Brain Amyloid Deposition. *JAMA* 2017;317(14):1443-50. doi: 10.1001/jama.2017.3090

34. Yassi N, Hilal S, Xia Y, et al. Influence of Comorbidity of Cerebrovascular Disease and Amyloid-beta on Alzheimer's Disease. *J Alzheimers Dis* 2020;73(3):897-907. doi: 10.3233/JAD-191028
35. Toledo JB, Arnold SE, Raible K, et al. Contribution of cerebrovascular disease in autopsy confirmed neurodegenerative disease cases in the National Alzheimer's Coordinating Centre. *Brain* 2013;136(Pt 9):2697-706. doi: 10.1093/brain/awt188
36. Wong TY, Knudtson MD, Klein R, et al. Computer-assisted measurement of retinal vessel diameters in the Beaver Dam Eye Study: methodology, correlation between eyes, and effect of refractive errors. *Ophthalmology* 2004;111(6):1183-90. doi: 10.1016/j.ophtha.2003.09.039
37. Cheung CY, Hsu W, Lee ML, et al. A new method to measure peripheral retinal vascular caliber over an extended area. *Microcirculation* 2010;17(7):495-503.
38. Hubbard LD, Brothers RJ, King WN, et al. Methods for evaluation of retinal microvascular abnormalities associated with hypertension/sclerosis in the Atherosclerosis Risk in Communities Study. *Ophthalmology* 1999;106(12):2269-80.
39. Frost S, Kanagasingam Y, Sohrabi H, et al. Retinal vascular biomarkers for early detection and monitoring of Alzheimer's disease. *Transl Psychiatry* 2013;3:e233. doi: 10.1038/tp.2012.150
40. Cheung CY, Ong YT, Ikram MK, et al. Microvascular network alterations in the retina of patients with Alzheimer's disease. *Alzheimers Dement* 2014;10(2):135-42. doi: 10.1016/j.jalz.2013.06.009
41. Williams MA, McGowan AJ, Cardwell CR, et al. Retinal microvascular network attenuation in Alzheimer's disease. *Alzheimer's & Dementia: Diagnosis, Assessment & Disease Monitoring* 2015;1(2):229-35. doi: <http://dx.doi.org/10.1016/j.dadm.2015.04.001>
42. Csincsik L, MacGillivray TJ, Flynn E, et al. Peripheral Retinal Imaging Biomarkers for Alzheimer's Disease: A Pilot Study. *Ophthalmic Res* 2018;59(4):182-92. doi: 10.1159/000487053
43. Cheung CY, Ong S, Ikram MK, et al. Retinal vascular fractal dimension is associated with cognitive dysfunction. *J Stroke Cerebrovasc Dis* 2014;23(1):43-50. doi: 10.1016/j.jstrokecerebrovasdis.2012.09.002
44. Ong YT, Hilal S, Cheung CY, et al. Retinal vascular fractals and cognitive impairment. *Dement Geriatr Cogn Dis Extra* 2014;4(2):305-13. doi: 10.1159/000363286
45. Hilal S, Ong YT, Cheung CY, et al. Microvascular network alterations in retina of subjects with cerebral small vessel disease. *Neurosci Lett* 2014;577:95-100. doi: 10.1016/j.neulet.2014.06.024

46. Cheung CY, Chen C, Wong TY. Ocular Fundus Photography as a Tool to Study Stroke and Dementia. *Semin Neurol* 2015;35(5):481-90. doi: 10.1055/s-0035-1563570
47. Jack CR, Jr., Holtzman DM. Biomarker modeling of Alzheimer's disease. *Neuron* 2013;80(6):1347-58. doi: 10.1016/j.neuron.2013.12.003
48. Ostergaard L, Engedal TS, Moreton F, et al. Cerebral small vessel disease: Capillary pathways to stroke and cognitive decline. *J Cereb Blood Flow Metab* 2016;36(2):302-25. doi: 10.1177/0271678X15606723
49. Ostergaard L, Aamand R, Gutierrez-Jimenez E, et al. The capillary dysfunction hypothesis of Alzheimer's disease. *Neurobiol Aging* 2013;34(4):1018-31. doi: 10.1016/j.neurobiolaging.2012.09.011
50. Kotliar K, Hauser C, Ortner M, et al. Altered neurovascular coupling as measured by optical imaging: a biomarker for Alzheimer's disease. *Sci Rep* 2017;7(1):12906. doi: 10.1038/s41598-017-13349-5
51. Golzan SM, Goozee K, Georgevsky D, et al. Retinal vascular and structural changes are associated with amyloid burden in the elderly: ophthalmic biomarkers of preclinical Alzheimer's disease. *Alzheimers Res Ther* 2017;9(1):13. doi: 10.1186/s13195-017-0239-9
52. de la Torre JC, Stefano GB. Evidence that Alzheimer's disease is a microvascular disorder: the role of constitutive nitric oxide. *Brain Res Brain Res Rev* 2000;34(3):119-36.
53. Yassine HN. Targeting prodromal Alzheimer's disease: too late for prevention? *Lancet Neurol* 2017;16(12):946-47. doi: 10.1016/S1474-4422(17)30372-1
54. Livingston G, Sommerlad A, Orgeta V, et al. Dementia prevention, intervention, and care. *Lancet* 2017;390(10113):2673-734. doi: 10.1016/S0140-6736(17)31363-6
55. Smith EE, Biessels GJ, De Guio F, et al. Harmonizing brain magnetic resonance imaging methods for vascular contributions to neurodegeneration. *Alzheimers Dement (Amst)* 2019;11:191-204. doi: 10.1016/j.dadm.2019.01.002
56. Humpel C. Identifying and validating biomarkers for Alzheimer's disease. *Trends Biotechnol* 2011;29(1):26-32. doi: 10.1016/j.tibtech.2010.09.007
57. Reid CM, Storey E, Wong TY, et al. Aspirin for the prevention of cognitive decline in the elderly: rationale and design of a neuro-vascular imaging study (ENVIS-ion). *BMC Neurol* 2012;12:3. doi: 10.1186/1471-2377-12-3
58. Palmqvist S, Janelidze S, Quiroz YT, et al. Discriminative Accuracy of Plasma Phospho-tau217 for Alzheimer Disease vs Other Neurodegenerative Disorders. *JAMA* 2020;324(8):772-81. doi: 10.1001/jama.2020.12134

59. Karikari TK, Pascoal TA, Ashton NJ, et al. Blood phosphorylated tau 181 as a biomarker for Alzheimer's disease: a diagnostic performance and prediction modelling study using data from four prospective cohorts. *Lancet Neurol* 2020;19(5):422-33. doi: 10.1016/S1474-4422(20)30071-5

## Figure Legends:

**Figure 1:** (A) Retinal photograph showing the optic nerve head, macular area, nerve fiber layer, arterioles and venules. (B) Examples of a cognitively normal subject; and (C) a subject with Alzheimer's disease (AD) dementia (global clinical dementia rating score of 1).

Retinal photographs assessed quantitatively with Singapore I Vessel Assessment software (SIVA, versions 4.0; National University of Singapore, Singapore). Arterioles are in red and venules are in blue. The measured area is standardized and defined as the region 0.5 to 2.0 disc diameters away from the disc margin. The subject with AD dementia was also diagnosed with age-related macular degeneration. The subject with AD dementia had a sparser retinal vascular network (arteriolar fractal dimension: 1.246 vs. 1.316; venular fractal dimension: 1.253 vs. 1.273) and more tortuous retinal vessels (arteriolar tortuosity ( $\times 10^4$ ): 0.61 vs. 0.48; venular tortuosity ( $\times 10^4$ ): 1.4 vs. 0.50), compared with the cognitively normal subject.

**Figure 2:** (A) Cross-sectional view of retina captured by optical coherence tomography (OCT). (B) Assessment of macular ganglion cell-inner plexiform layer (GC-IPL) and (C) peripapillary retinal nerve fibre layer (RNFL) of a subject who presented with mild cognitive impairment having a positive cerebral amyloid PET imaging, measured with Cirrus HD-OCT (Carl Zeiss Meditec, Inc., Dublin, CA, USA) (OD=right eye; OS=left eye). No retinal disorders were observed in this subject. The GC-IPL thickness map (B) and peripapillary RNFL thickness map (C) uses a false colour coding with warm colours represent high and cool colours represent low thickness values. The software further compares the measured thickness to the device's internal normative age-matched database, and generates a deviation map. Thinner GC-IPL and RNFL thicknesses are observed in this example in prodromal stage. (D) A cross-sectional view of choroidal vasculature in an example of a cognitively normal subject; and (E) in a subject with

Alzheimer's disease (AD) dementia (global clinical dementia rating score of 1). The choroid is indicated by red arrows. Choroidal-scleral interface can be clearly identified. The subject with AD dementia had a thinner choroidal layer, compared with the cognitively normal subject.

**Figure 3.** Imaging of retinal capillary network using optical coherence tomography angiography (OCTA), which is not visualized using conventional retinal camera.

**Box 1.** Similarities between the retina and the brain.

***Embryological***

- During embryonic development, the retina and optic nerve originate from the diencephalon. The retina maintains its connection with the brain via the optic nerve after birth, being an integral component of the CNS.<sup>12</sup>

***Anatomical***

- Anatomically, the layered cytological and vascular structures and the presence of a blood barrier are similar in the retina and the brain. The retinal layers are composed of several types of neurons including the retinal ganglion cell (RGC) which comprises a cell body, dendrites and an axon, similar to neurons in the CNS. In addition, the RGCs axons, which collectively form the optic nerve, are myelinated by oligodendrocytes and are ensheathed by all three layers of meninges. Furthermore, the retinal tissue is isolated by the blood-retinal barrier which maintains a distinct immunological and physiological environment, similar to the blood-brain barrier.<sup>S153</sup> In terms of vascular structure, both the cerebral and the retinal microvasculature components are surrounded by a single layer of endothelial cells, which are non-fenestrated and possess similar intercellular tight junctional complexes.<sup>S154</sup> Both are also surrounded by the perivascular end feet from astrocytes.<sup>S155</sup> The choroid, the primary vascular supply for the outer retina, is sandwiched between the retina and the sclera. This has one of the highest blood flows per volume unit of any structure in the body.

***Physiological***

- There are many physiological similarities between retina and brain. First, a NVU is present in both retina and brain, widely known as the “blood-retinal barrier” and “blood-brain barrier”, respectively.<sup>13, S156</sup> The NVU allows functional coupling and interdependency of neurons, glia and the vasculature, for example, regulating blood flow in response to neural activity or metabolic demands.<sup>S157,S158</sup> Retinal vascular autoregulation is achieved by retinal glial-synaptic

interaction.<sup>S158</sup> Second, similar to the CNS neurons, the RGCs produce an identical response to insults, including axonal degeneration, myelin destruction, scar formation, and secondary degeneration.<sup>S159-S161</sup> In addition, the RGCs have limited regenerative ability after injury.<sup>S162</sup> Third, the retina is considered an immune-privileged site and contain similar collection of cell-surface molecules, immunoregulatory molecules and cytokines.<sup>S163,S164</sup> Moreover, both cerebral and retinal microglia show phagocytic properties and phagocytose injured neurons.<sup>S165,S166</sup> The cerebral vasculature is devoid of autonomic innervation beyond the pia vessels.<sup>S167</sup> Similarly, there is no autonomic innervation to the retinal vasculature beyond the level of the lamina cribrosa (except the choroidal circulation).<sup>S168,S169</sup> Finally, both the inner retinal and the cerebral circulation are under the fine control of the autoregulatory mechanism, which consists of myogenic and metabolic components.<sup>S154</sup>

**Table 1:** Glossary of retinal imaging technologies and parameters used in studying Alzheimer's disease.

Retinal imaging technologies	Parameters measured from retinal imaging	Descriptions of the parameters
Spectral-domain optical coherence tomography (SD-OCT)	Peripapillary retinal nerve fiber layer (RNFL) thickness	A thickness of RNFL layer in peripapillary region to assess retinal ganglion cell (RGC) axon. Traditionally, peripapillary RNFL thickness is calculated along a 3.4 mm circle around optic disc.
	Macular ganglion cell inner plexiform layer (GC-IPL) thickness	A combined thickness of ganglion cell layer and inner plexiform layer in macular region to assess RGC cell bodies and dendrites.
	Macular ganglion cell complex (GCC) layer	A combined thickness of RNFL, ganglion cell layer and inner plexiform layer in macular region to assess RGC axon, cell bodies and dendrites.
	Macular thickness or volume	A thickness or volume between inner limiting membrane and the retinal pigment epithelium at macular region.
Quantitative retinal vasculature analysis with retinal fundus photography	Central retinal artery equivalent (CRAE)	A summary index reflecting the average width of retinal arterioles.
	Central retinal venule equivalent (CRVE)	A summary index reflecting the average width of retinal venules.
	Fractal dimension	A measure of a fractal structure, that exhibits the property of self-similarity, characterizing the distribution of the branching retinal vasculature.
	Tortuosity	A measure of the straightness/curliness of the retinal vessels.
	Length-diameter-ratio	A measure of the ratio of the length between 2 branching points to trunk vessel width.
Optical coherence tomography angiography (OCT-A)	Vessel density	A measure of the area occupied by blood vessels (including capillaries) over total area within the interested region.

	Foveal avascular zone (FAZ) area	A capillary-free area in the central macula with highest cone photoreceptor density and oxygen consumption.
Optical coherence tomography with enhanced depth imaging (OCT-EDI)	Choroidal thickness or volume	A thickness or volume between the outer border of retina pigment epithelium and sclera-choroidal interface.
Dynamic vessel analyzer	Flicker-induced vessel dilation	An average percentage increase in the vessel diameter in response to the flickering-light during measurement cycles, relative to the baseline diameter size.
Retinal oximetry	Retinal vessel oxygen saturation	A measure of the oxygen saturation in retinal arterioles and venules to detect changes in oxygen metabolism.
Ultra-widefield retinal photography	Presence of peripheral hard drusen	Presence of small and distinct yellow deposits under retina in the periphery.
Fluorescence lifetime imaging ophthalmoscopy (FLIO)	Fluorescence lifetime	A measure to describe the average time a single fluorophore remains in its electronically excited state after absorbing the energy of a photon and before returning to the ground state by emitting a photon.

**Table 2.** The summary of current findings on retinal neuronal changes, retinal capillary changes, retinal arteriolar and venular changes, and choroidal vasculature changes.

	<b>Preclinical AD or MCI</b>	<b>AD dementia</b>
<b>Retinal Neuronal Changes</b>		
Peripapillary RNFL Thickness	<ul style="list-style-type: none"> <li>• Some studies showed reduced peripapillary RNFL, macular GC-IPL and GCC thicknesses, compared with controls</li> <li>• But a few studies showed no differences in the measures, compared with controls and AD dementia</li> <li>• A few studies also showed thickened peripapillary RNFL and macular GC-IPL thicknesses in MCI, compared with controls</li> </ul>	<ul style="list-style-type: none"> <li>• Majority of studies and meta- analysis showed reduced peripapillary RNFL, macular GC-IPL and macular thicknesses, compared with controls</li> <li>• But a few studies showed no differences in the measures, compare with controls</li> <li>• A few studies also showed thickened peripapillary RNFL and macular GC-IPL thicknesses, compared with controls</li> <li>• In a population-based study, reduced peripapillary associated with incident AD dementia</li> </ul>
<b>Retinal Capillary Changes</b>		
Vessel density and foveal avascular zone	<ul style="list-style-type: none"> <li>• Majority of studies showed decreased vessel density and enlarged foveal avascular zone area, compared with controls</li> <li>• But a few studies showed no differences in the measures, and one study showed increased vessel density in preclinical AD, compared with controls.</li> </ul>	<ul style="list-style-type: none"> <li>• Majority of studies showed decreased vessel density and enlarged foveal avascular zone area, compared with controls</li> <li>• But a few studies showed no differences in the measures.</li> </ul>
<b>Retinal Arteriolar and Venular Changes</b>		
Vessel caliber (CRAE and CRVE)	<ul style="list-style-type: none"> <li>• No data</li> </ul>	<ul style="list-style-type: none"> <li>• Majority of studies showed narrower CRVE, compared with controls.</li> </ul>

Fractal dimension	<ul style="list-style-type: none"> <li>• No data</li> </ul>	<ul style="list-style-type: none"> <li>• Majority of studies showed decreased arteriolar and venular fractal dimensions, compared with controls.</li> </ul>
Tortuosity	<ul style="list-style-type: none"> <li>• No data</li> </ul>	<ul style="list-style-type: none"> <li>• The association is equivocal. Both increased and decreased retinal vascular tortuosity were observed.</li> </ul>
<b>Choroidal vasculature changes</b>		
Choroidal thickness	<ul style="list-style-type: none"> <li>• No data</li> </ul>	<ul style="list-style-type: none"> <li>• Reduced choroidal thicknesses, compared with controls</li> <li>• A larger reduction in choroidal thicknesses over a 12-month follow-up, compared with controls.</li> </ul>

CRAE=central retinal artery equivalent; CRVE=central retinal vein equivalent; GCC=ganglion cell complex; GC-IPL=ganglion cell-inner plexiform layer; MCI=mild cognitive impairment; RNFL=retinal nerve fiber layer.

## **Supplementary Section 1. Details of Retinal Imaging Technology for Specific Structures**

### 1. Spectral-domain optical coherence tomography for imaging retinal neuronal and axonal layers

Optical coherence tomography (OCT) is an optical imaging technique that utilises a low-coherence light source near the infra-red spectrum to penetrate biological tissue and provides cross-sectional imaging of the retinal layered structure.<sup>S170</sup> Spectral-domain OCT (SD-OCT) employs a spectrometer to analyse the interference spectrum data from the back-scattered light which includes the retina depth information and generate axial measurements of the retina.<sup>S35</sup> Comparing with the earlier generation of OCT (time-domain OCT) which collected the signal as a function of time by moving a reference mirror mechanically, SD-OCT with the spectral analysis provides a higher resolution and higher speed for imaging the retinal layered structure.<sup>S35</sup> The recent development of swept-source OCT (SS-OCT), with a longer wavelength ( $>1\mu\text{m}$ ) than SD-OCT and utilizing a frequency-swept light source, further enhances tissue penetration into the choroid and provides a faster scanning speed.<sup>S171,S172</sup>

Assessment of inner retinal layers in greater details is possible after the development of SD-OCT, in particular the ganglion cell layer and inner-plexiform layer, which indicate cell bodies and dendrites of retinal ganglion cells (RGCs), respectively.<sup>S173</sup> Retinal layers (e.g. inner limiting membrane, nerve fibre layer, ganglion cell layer, inner plexiform layer and retinal pigment epithelium) are segmented automatically for different thickness and volume measurements (e.g. retinal nerve fibre layer (RNFL) thickness, ganglion cell-inner plexiform layer (GC-IPL) thickness, macular thickness and macular volume) at different locations by built-in segmentation algorithms in commercial OCT systems.

In addition to thickness measurement, built-in normative databases from healthy subjects are also provided for comparing the measured thickness or volume to age-matched data. The normative database uses a colour code to indicate the normal distribution percentiles (red: <1%, below normal limits; yellow: within 1% to 5%, suspect below normal; green: within 5%-95%, normal limits; light yellow: within 95%-99%, above normal limits; light red: >99%, above normal limits). For example, areas flagged in red indicate significant thickness reduction, compared with normative database.

## 2. Optical coherence tomography angiography for imaging retinal capillary networks

Optical coherence tomography-angiography (OCT-A) is based on mapping red blood cells movement over time from volumetric OCT scans.<sup>S65</sup> At each cross-sectional OCT image position, scan is repeated few times in order to detect and quantify the motion contrast. The degree of motion contrast is corresponding to angiographic flow, as the only expected motion in the retina is blood flow in vessels. Based on different image processing algorithms such as OCT Angiography Ratio Analysis (OCTARA),<sup>S174</sup> split-spectrum amplitude-decorrelation angiography (SSADA)<sup>S64</sup> and optical microangiography (OMAG) algorithm,<sup>S175</sup> OCT-angiography is able to penetrate into the retinal layers and image the various different capillary plexuses by selecting different *en face* slabs, thereby providing us the unique ability to reconstruct and view the retinal vasculature in a 3-dimensional fashion, as well as to visualize in isolation the individual retinal plexuses without intravenous dye injection (e.g. the superficial capillary plexus and deep capillary plexus).

It is noteworthy that the definition of “segmentation of retinal capillary plexuses” vary in different algorithms. For example, in the OCTARA, at macular region, the superficial capillary plexus default segmentation is defined as the region between the inner limiting membrane (ILM) + 2.6

$\mu\text{m}$  to the inner plexiform layer (IPL)/ inner nuclear layer (INL) border + 15.6  $\mu\text{m}$ , while the deep capillary plexus default segmentation is defined as the region from the IPL/INL border + 15.6  $\mu\text{m}$  to the IPL/INL border + 70.2  $\mu\text{m}$ . In the SSASD, the superficial capillary plexus upper border is at 3  $\mu\text{m}$  below ILM to the lower border at 15  $\mu\text{m}$  below the IPL, while the deep capillary plexus spans from 15  $\mu\text{m}$  below the IPL to 70  $\mu\text{m}$  below the IPL.<sup>S176</sup>

Quantification of capillary network from OCT-A to identify early and subtle microvascular changes objectively is one of the next important milestones for the application of OCT-A into clinical practice. Currently, several quantitative OCT-A measurements (e.g. vessel density, foveal avascular zone area and circularity, fractal dimension, vessel density index) have been defined and different automated and semi-automated algorithms developed to quantify the capillary networks.<sup>S63, S64, S177</sup> It is noted that projection artifacts from superficial blood vessels on the deeper layers (a fluctuating shadow cast by the flowing blood cells in the overlying retinal vessels projecting to the deeper layers) are common, which may lead to incorrect interpretations.<sup>S178</sup>

### 3. Enhanced depth imaging OCT for imaging choroidal vasculature

The choroid is the posterior part of the eyeball, which is sandwiched between the retina and the sclera, and is one of the most vascularized structures in the human body. Although SD-OCT can image the layered retina in details, imaging the choroid with SD-OCT is impeded by poor signal penetration beyond the heavily pigmented retinal pigment epithelium.<sup>S179</sup> With the introduction of enhanced depth imaging (EDI) technique of SD-OCT, the visualization of choroidal scleral interface is enhanced and imaging of choroidal vasculature has become possible.<sup>S179</sup> SS-OCT with a longer wavelength than SD-OCT, reducing the scatter reflection of the retinal pigment epithelium, also enables a better imaging of choroidal vasculature.<sup>S171, S172</sup> The thickness and volume of the

choroid at different regions (e.g. subfovea, macula, peripapillary) can be subsequently measured by computer software.<sup>S104,S180</sup> It is noteworthy that choroidal thickness is associated with several physiological variables (e.g. age, axial length of eyeball, intraocular pressure) in normal individuals.<sup>S181</sup> Choroidal vascularity index, defined as the ratio of vascular area to the total choroidal area, is recently proposed to quantify choroidal vascular alterations in a more reliable manner as it has lesser variability and influence by these factors.<sup>S182</sup>

#### 4. Retinal vasculature analysis with retinal photography for imaging and quantifying retinal vasculature

The optical design of retinal photography with fundus camera is based on the principle of monocular indirect ophthalmoscopy, with the pupil used as both an entrance and exit for the fundus camera's illuminating and imaging light rays. With advancements in digital retinal photography and image processing technologies, quantitative retinal vasculature analysis from retinal photographs can be performed with computer software and standardized photographic protocols. Retinal Analysis (RA; University of Wisconsin, Madison, WI) and Integrative Vessel Analysis (IVAN; University of Wisconsin, Madison; WI) were widely used for measuring retinal arteriolar caliber and retinal venular caliber from retinal photographs in numerous large population-based studies.<sup>S183,S184</sup> Retinal vessels, coursing through a specified area of a standardized grid (0.5–1.0 disc diameter from the disc margin), are measured. The revised Knudtson-Parr-Hubbard formula is widely used to summarize the retinal arteriolar and venular calibers of the large six arterioles and venules as central retinal artery equivalent (CRAE) and central retinal vein equivalent (CRVE) respectively.<sup>S185</sup> Subsequently, newer retinal geometric branching parameters were defined to quantify the optimal state of retinal vasculature in recent computer software systems (e.g. SIVA

(Singapore I Vessel Assessment) software<sup>S103,S186</sup> and VAMPIRE software (Vascular Assessment and Measurement Platform for Images of the REtina))<sup>S61</sup> measured from a wider measured area, based on Murray's principle that the branching pattern of vascular networks develops to minimize the energy required to maintain efficient blood flow.<sup>S53</sup> It is noted that the current retinal vasculature analysis software tools are mainly semi-automated, and require manual adjustment and assessment usually by trained technicians to maximise the accuracy of the measurements.

#### 5. Dynamic vessel analyzer for measuring the flicker-induced vasodilatory response

The principle of dynamic vessel analyzer (DVA) is based on dynamic reaction of retinal vessels to flickering light which stimulates activity of the neural retina and leads to retinal vessel dilation influenced by neurovascular coupling. In order to generate flickering light during DVA imaging, an optoelectric shutter is inserted in a retinal camera to produce a bright-to-dark contrast ratio of at least 25:1.<sup>S187</sup> In each imaging cycle, retinal arteriolar and venular diameters are firstly measured in a certain time period for baseline measurement, followed by a stimulation with flickering light of the same wavelength for another time period, and then a non-flicker period. The responses to flickering light can be represented as an average increase in the retinal arteriolar and venular diameters during several cycles, and defined as the percentage increase relative to the baseline diameter size.<sup>S84</sup>

#### 6. Retinal oximetry for measuring retinal vessel oxygen saturation

Retinal oximeter, composed of an optical adapter and an image splitter fitted to a fundus camera, measures retinal vessel oxygen saturation based on acquisition of two images of the same area of the retinal fundus at two different wavelengths of light simultaneously. One of the two wavelengths

is sensitive to oxygen saturation (isosbestic wavelength of 570nm), i.e. the light absorbance changes with the oxygen saturation, while the other is insensitive to oxygen saturation (non-isosbestic wavelength of 600nm) and is used to calibrate the light intensity. The oxygen saturation can therefore be estimated by comparing light absorption at oxygen sensitive wavelengths for assessing retinal oxygen metabolism.<sup>S87</sup> Nevertheless, the choroid may have a considerable role in oxygenating the inner retina under some circumstances (e.g. 100% oxygen breathing), but this is not accounted for in the current estimation of haemoglobin oxygen saturation.<sup>S87</sup>

#### 7. Ultra-wide field retinal photography for imaging the retinal periphery

The technology of ultra-wide field retinal photography is based on confocal laser scanning microscopy combined with a concave ellipsoidal mirror, or white-light light-emitting diode illuminator, which enable a wide field of view to be imaged without the need for pupillary dilation.<sup>S188</sup> Ultra-wide field retinal photography has the ability to capture a much wider view of the retina (up to 200° horizontally or 82% of the retina) in a single image for assessment of peripheral lesions (e.g. drusen deposits, diabetic retinopathy), compared with conventional retinal photography (30° to 50° of the retina).<sup>S189,S190</sup> The confocal laser scanning microscopy based system can allow for fundus autofluorescence imaging at the same time.<sup>S191</sup> It is noted that images from the confocal laser scanning microscopy can only produce pseudo-color images, but not true colour imaging like conventional fundus photography.

#### 8. Fluorescence lifetime imaging ophthalmology for measuring and quantifying lifetimes of retinal fluorophore

Retinal fluorophores, including lipofuscin, advanced glycation end products, collagen, melanin, and elastin, absorb and emit light at specific wavelengths. Electrons in retinal fluorophores are excited by absorbing photons from a monochromatic light source (e.g. laser), thus moving to a higher level of energy. They return to their energy ground state by emitting photons of longer wavelengths than the exciting light. Fluorescence lifetime imaging ophthalmoscope (FLIO) is based on a commercial scanning laser ophthalmoscope which is equipped with an infrared camera for active eye tracking to correct for eye movements.<sup>S94</sup> During imaging, the excitation laser raster scans the retina in multiple periods, detects the emitted fluorophore and builds up a distribution histogram over time. The fluorescence lifetime describes the average time a single fluorophore remains in its electronically excited state after absorbing the energy of a photon and before returning to the ground state by emitting a photon. Every fluorophore is characterized by its own excitation and emission wavelength spectrum and exhibits an individual fluorescence lifetime. Therefore, it can produce quantitative images based on the lifetimes of the different retinal fluorophores.<sup>S191</sup>

**Supplementary Table 1.** Recent clinical studies of common primary age-related ocular diseases and Alzheimer’s diseases (AD) dementia.

Clinical retinal diseases	Authors, years	Sample	Summary of results
<b><u>Age-related macular degeneration (AMD)</u></b>			
	Keenan et al. (2014) <sup>S2</sup>	Record linkage data of English National Health Service: an AMD cohort of 65,894 persons, a dementia cohort of 168, 092 persons and a reference cohort of 7.7 million persons.	<ul style="list-style-type: none"> <li>• For people with AMD: the rate ratio, comparing observed and expected cases of dementia in the AMD cohort with those of the reference cohort, was 0.91 (0.79, 1.04). The rate ratio for AD dementia after AMD was 0.86 (0.67, 1.08).</li> <li>• Persons with AMD not associated with incident dementia (RR: 0.91 [0.79,1.04]) or AD dementia (RR: 0.86 [0.67-1.08]), compared with the reference cohort.</li> <li>• Persons with any forms of dementia (RR: 0.07 [0.04, 0.11]) and persons with AD dementia (RR: 0.04 [0.01,0.10]) were unlikely to develop AMD, compared with the reference cohort.</li> </ul>
	Williams et al. (2014) <sup>S3</sup>	258 AD dementia, and 322 healthy control subjects	<ul style="list-style-type: none"> <li>• AMD grades not associated with AD dementia, compare with AMD Grade 0 (Grade 1: OR: 0.65 [0.4–1.1]; Grade 2: OR: 1.00 [0.5–1.9]; Grade 3: OR: 1.38 [0.6–3.2]).</li> </ul>
	Tsai et al. (2015) <sup>S4</sup>	Claims data of the Taiwan National Health Insurance Research Database: an AMD cohort of 4,993 person (4,453 non-exudative AMD and 540 exudative AMD) and an age-gender-matched reference cohort of 24,965 persons.	<ul style="list-style-type: none"> <li>• 5.9% and 5.2% persons were diagnosed with AD or senile dementia during a mean follow-up period of 4.4 years in the AMD cohort and the control cohort, respectively.</li> <li>• Persons with AMD were more likely to develop AD dementia or senile dementia (HR: 1.44 [1.26, 1.64]), compared with controls.</li> <li>• The association was stronger in non-exudative AMD (HR:1.44 [1.26, 1.65]).</li> </ul>
	Lee et al. (2018) <sup>S5</sup>	3,877 participants with dementia-free at enrollment from the Adult Changes in Thought Study	<ul style="list-style-type: none"> <li>• 347 (9%) had an AMD diagnosis at enrollment, and 689 (18%) developed AMD</li> <li>• Established AMD (&gt;5 years) associated with incident AD dementia (HR: 1.50 [1.25, 1.8]).</li> </ul>
<b><u>Diabetic retinopathy (DR)</u></b>			

	Lee et al. (2018) <sup>S5</sup>	3,877 participants with dementia-free at enrollment from the Adult Changes in Thought Study	<ul style="list-style-type: none"> <li>• 136 (4%) had a DR diagnosis at enrollment, and 112 (3%) developed DR.</li> <li>• Both recent DR (within 5 years) (HR: 1.67 [1.01, 2.74]) and established DR (&gt;5 years) (HR: 1.50 [1.05, 2.15]) associated with incident AD dementia.</li> </ul>
<b><u>Glaucoma</u></b>			
	Lin et al. (2014) <sup>S6</sup>	Claims data of the Taiwan National Health Insurance Research Database: a primary open-angle glaucoma (POAG) cohort of 3,979 persons and a non-glaucoma cohort of 15,916 persons	<ul style="list-style-type: none"> <li>• The incidence rates of AD dementia among the patients with and without POAG were 2.85 (2.19, 3.70) and 1.98 (1.68, 2.31) per 1000 person-years, respectively.</li> <li>• Persons with POAG were more likely to develop AD dementia (HR: 1.40 [1.03, 1.90]), but not Parkinson disease (HR: 0.98 [0.77, 1.24]), over 8 years, compared with non-glaucoma cohort.</li> </ul>
	Keenan et al. (2015) <sup>S7</sup>	Record linkage data of English National Health Service: a POAG cohort of 87,658 persons, an AD dementia cohort of 251,703 persons, a vascular dementia cohort of 217,302 persons and a reference cohort of >2.5 million persons.	<ul style="list-style-type: none"> <li>• For people with POAG, there was no significant association with AD: the rate ratio, comparing the POAG cohort with the reference cohort, was 1.01 (0.96, 1.06). The rate ratio for AD dementia after AMD was 0.86 (0.67, 1.08).</li> <li>• Persons with POAG not associated with incident AD dementia (RR:1.01 [0.96, 1.06]), but likely to develop vascular dementia (RR: 1.10 [1.05 to 1.16]), compared with the reference cohort.</li> <li>• Persons with AD dementia (RR: 0.28 [0.24 to 0.31]) or vascular dementia (RR: 0.32 [0.28 to 0.37]), were unlikely to develop POAG, compared with the reference cohort.</li> </ul>
	Lee et al. (2018) <sup>S5</sup>	3,877 participants from the Adult Changes in Thought Study	<ul style="list-style-type: none"> <li>• 404 (10%) had a glaucoma diagnosis at enrollment, and 290 (7%) developed glaucoma.</li> <li>• Recent glaucoma (within 5 years) associated with incident AD dementia (HR: 1.46 [1.08, 1.91]).</li> </ul>

A $\beta$ =amyloid-beta; AD=Alzheimer's disease; HR= hazard ratio; OR=odds ratio; RNFL= retinal nerve fiber layer; RR= relative risk; PET=positron emission tomography.

**Supplementary Table 2.** Recent clinical studies of spectrum of Alzheimer’s diseases (AD) (AD dementia, mild cognitive impairment (AD MCI), preclinical AD), and retinal imaging measures, as defined from spectral-domain optical coherence tomography (SD-OCT), OCT-angiography, enhanced depth imaging (EDI) with OCT and retinal photography. It is noted that the definition of AD varies in the existing literature: not all publications have included AD biomarkers for their AD diagnosis. The evolution in definition and diagnostic criteria of AD and other dementias may account for some of the variations and differences seen between studies discussed in this review.

Authors, years	Sample	Imaging measure	Summary of results
<b><u>Cross-sectional SD-OCT studies</u></b>			
Larrosa et al. (2014) <sup>S193</sup>	151 AD dementia, and 61 age-matched normal control subjects	A selective combination of peripapillary RNFL and macular thicknesses using linear discriminant function	<ul style="list-style-type: none"> <li>• Reduced peripapillary RNFL thickness using linear discriminant function in AD dementia (all <math>p &lt; 0.001</math>), compared with controls.</li> <li>• The largest AUROCs were 0.967 for the Spectralis RNFL based linear discriminant function and 0.830 for the Cirrus RNFL based linear discriminant function.</li> </ul>
Polo et al. (2014) <sup>S194</sup>	75 AD dementia, and 75 age-matched normal control subjects	Peripapillary RNFL and macular thickness	<ul style="list-style-type: none"> <li>• Reduced peripapillary RNFL in superior (<math>113.59\mu\text{m}</math> vs. <math>118.58\mu\text{m}</math>, <math>p=0.006</math>) and inferior (<math>121.96\mu\text{m}</math> vs. <math>127.97\mu\text{m}</math>, <math>p=0.018</math>) quadrants, and macular thicknesses (all <math>p \leq 0.009</math>, except measurement at fovea [<math>p=0.115</math>]) in AD dementia, compared with controls.</li> </ul>
Cheung et al. (2015) <sup>20</sup>	100 AD dementia, 41 MCI, and 123 normal control subjects	Macular GC-IPL and Peripapillary RNFL thicknesses	<ul style="list-style-type: none"> <li>• Reduced macular GC-IPL thickness in MCI (all <math>p \leq 0.049</math>, except measurement at superior [<math>p=0.064</math>], inferonasal [<math>p=0.051</math>] and supertemporal [<math>p=0.359</math>] sectors) in AD dementia (all <math>p \leq 0.031</math>), compared with controls.</li> <li>• Reduced peripapillary RNFL thickness in superior quadrant in AD dementia (<math>109.1\mu\text{m}</math> vs. <math>111.1\mu\text{m}</math>, <math>p=0.039</math>), compared with controls.</li> <li>• No difference in macular GC-IPL and peripapillary RNFL thicknesses between MCI and AD dementia.</li> </ul>
Ferrari et al. (2016) <sup>S195</sup>	39 AD dementia, 17 frontotemporal dementia (FTD), 27 MCI and 49 normal control subjects	Peripapillary RNFL and GC-IPL thicknesses	<ul style="list-style-type: none"> <li>• Reduced peripapillary RNFL and GC-IPL thicknesses in AD dementia (mild AD: RNFL=<math>94.55\mu\text{m}</math>, GCIPL=<math>57.52\mu\text{m}</math>; moderate AD: RNFL=<math>91.33\mu\text{m}</math>, GCIPL=<math>50.07\mu\text{m}</math>), FTD (RNFL=<math>87.47\mu\text{m}</math>, GCIPL=<math>51.83\mu\text{m}</math>) and MCI (RNFL=<math>92.79\mu\text{m}</math>,</li> </ul>

			GCIPL=55.61 $\mu\text{m}$ ) (all $p < 0.05$ ), compared with controls (RNFL=97.49 $\mu\text{m}$ , GCIPL=58.18 $\mu\text{m}$ ).
Garcia-Martin et al. (2016) <sup>S196</sup>	150 AD dementia and 75 age-gender-matched normal control subjects	Macular RNFL, GCL, IPL, INL, OPL, ONL, RPE layer and photoreceptor layer thicknesses	<ul style="list-style-type: none"> <li>• Reduced macular RNFL (6.11 vs. 6.22), GCL (6.27 vs. 6.45), INL (6.56 vs. 6.71) and ONL (6.56 vs. 6.71) thicknesses in AD dementia (<math>p &lt; 0.050</math>), compared with controls.</li> <li>• Reduced RNFL (<math>p = 0.018</math>), GCL (<math>p = 0.009</math>) and INL (<math>p = 0.006</math>) thicknesses correlated with disease duration in AD dementia.</li> </ul>
Snyder et al. (2016) <sup>S39</sup>	10 A $\beta$ -positive and 53 A $\beta$ -negative subjects at high-risk for AD (self-reported first-degree family history of the disease, and self-identification of subjective memory concerns)	Peripapillary RNFL and macular RNFL, GCL, IPL, INL, OPL, and ONL thicknesses.	<ul style="list-style-type: none"> <li>• Increased IPL in A<math>\beta</math>-positive group (<math>p = 0.029</math>), compared with A<math>\beta</math>-negative group (0.371<math>\mu\text{m}^3</math> vs. 0.354 <math>\mu\text{m}^3</math>).</li> </ul>
Cunha et al. (2017) <sup>S197</sup>	50 mild AD dementia and 152 normal control subjects	Peripapillary RNFL and macular thicknesses	<ul style="list-style-type: none"> <li>• Reduced peripapillary RNFL thickness in superiotemporal sector (<math>p &lt; 0.05</math>) and macular thicknesses in pericentral (<math>p = 0.001</math>) and peripheral superior (<math>p &lt; 0.001</math>) sectors in AD dementia, compared with controls.</li> </ul>
Lad et al. (2018) <sup>S38</sup>	15 AD dementia, 15 MCI and 18 normal control subjects	Peripapillary RNFL and macular RNFL and GC-IPL thicknesses	<ul style="list-style-type: none"> <li>• No significant associations observed.</li> <li>• Using a multivariate regression model with quasi-least squares, there are areas of thickening of macular GC-IPL and RNFL in subjects with AD dementia and MCI, compares with controls.</li> </ul>
O'Bryhim et al. (2018) <sup>S74</sup>	14 preclinical AD (A $\beta$ -positive from PET or CSF but not dementia) and 16 normal control subjects	Inner, outer, and total foveal thicknesses	<ul style="list-style-type: none"> <li>• Reduced inner foveal thickness (66.0<math>\mu\text{m}</math> vs. 75.4<math>\mu\text{m}</math>, <math>p = 0.03</math>) in preclinical AD, compared with controls.</li> </ul>
Sanchez et al. (2018) <sup>17</sup>	324 AD dementia, 192 MCI and 414 normal control subjects	Peripapillary RNFL thickness	<ul style="list-style-type: none"> <li>• No difference in peripapillary RNFL thickness among the groups.</li> </ul>
den Haan et al. (2019) <sup>S42</sup>	57 AD dementia and 85 normal control subjects	Peripapillary RNFL, total macular and macular RNFL, GCL and IPL thicknesses	<ul style="list-style-type: none"> <li>• No difference in peripapillary RNFL, total macular and macular RNFL, GCL and IPL thicknesses among the groups.</li> </ul>

Tao et al. (2019) <sup>26</sup>	73 AD dementia, 51 MCI and 67 normal control subjects	Peripapillary RNFL and macular GCC thicknesses	<ul style="list-style-type: none"> <li>• Reduced peripapillary RNFL (97.99<math>\mu</math>m vs. 98.35<math>\mu</math>m vs. 107.19<math>\mu</math>m) and macular GCC thicknesses (94.16<math>\mu</math>m vs. 94.1<math>\mu</math>m vs. 99.64<math>\mu</math>m) in AD dementia and MCI (all <math>p &lt; 0.05</math>), compared with controls.</li> <li>• No difference in peripapillary RNFL and macular GCC thicknesses between MCI and AD dementia.</li> </ul>
Asanad et al. (2020) <sup>198</sup>	27 preclinical AD (pathological A $\beta$ 42/Tau ratio from CSF but not dementia) and 16 normal control subjects	Peripapillary RNFL, macular GC-IPL and macular thicknesses	<ul style="list-style-type: none"> <li>• Reduced peripapillary RNFL thicknesses in preclinical AD dementia (83.46<math>\mu</math>m vs. 93.27<math>\mu</math>m, <math>p = 0.0009</math>), compared with controls.</li> </ul>
McCann et al. (2020) <sup>199</sup>	3,221 subjects from the Northern Ireland Cohort for the Longitudinal Study of Ageing (NICOLA)	Peripapillary RNFL thickness	<ul style="list-style-type: none"> <li>• Reduced associated with AD (self-reported) in the age-adjusted and sex-adjusted model.</li> </ul>
<b><u>Prospective SD-OCT studies</u></b>			
Shi et al. (2014) <sup>29</sup>	20 MCI and 58 normal control subjects	Peripapillary RNFL thickness	<ul style="list-style-type: none"> <li>• The reduction in peripapillary RNFL at inferior region in the converted participants was greater than that in stable participants (-11.0<math>\mu</math>m vs 0.4<math>\mu</math>m, <math>p = 0.009</math>) over a 25-month follow-up.</li> </ul>
Trebbastoni et al. (2016) <sup>31</sup>	36 AD dementia and 36 age-matched normal control subjects	Peripapillary RNFL thickness	<ul style="list-style-type: none"> <li>• Changes in peripapillary RNFL thickness in inferior region associated with worsening cognitive scores (ADAS-Cog scores change: <math>r = -0.35</math>, <math>p = 0.02</math>; CDR scores change: <math>r = -0.39</math>, <math>p = 0.008</math>) over a 12-month follow-up.</li> </ul>
Choi et al. (2016) <sup>30</sup>	42 AD dementia, 26 MCI and 66 normal control subjects	Peripapillary RNFL, macular GC-IPL and macular thicknesses	<ul style="list-style-type: none"> <li>• Reduced average (Beta=-0.150, <math>p = 0.006</math>) and sectoral GC-IPL (all <math>p &lt; 0.05</math>) and macular (Beta=-1.700, <math>p = 0.02</math>) thicknesses at baseline associated with progression of AD dementia and MCI over a 2-year follow-up.</li> </ul>
Mutlu et al. (2018) <sup>27</sup>	3,289 subjects from the Rotterdam Study	Peripapillary RNFL and macular GC-IPL thicknesses	<ul style="list-style-type: none"> <li>• Reduced GC-IPL (OR: 1.03 [1.00, 1.09]) associated with prevalent dementia.</li> <li>• Reduced RNFL (HR: 1.02 [1.01, 1.04]) associated with incident of dementia, including AD dementia (HR: 1.02 [1.01, 1.04]).</li> </ul>

Santos et al. (2018) <sup>S200</sup>	15 preclinical AD and 41 normal control subjects	Peripapillary RNFL and macular RNFL, GCL, IPL, INL, OPL, and ONL thicknesses.	<ul style="list-style-type: none"> <li>• A larger reduction in macular RNFL (-0.032mm<sup>3</sup> vs. -0.019mm<sup>3</sup>, p=0.050), ONL (-0.029mm<sup>3</sup> vs. -0.007mm<sup>3</sup>, p=0.026), and IPL (-0.014mm<sup>3</sup> vs. -0.006mm<sup>3</sup>, p=0.020) volumes, in preclinical AD over a 27-month follow-up, compared with controls.</li> </ul>
<b><u>OCT-angiography studies</u></b>			
Jiang et al. (2018) <sup>S68</sup>	12 AD dementia, 19 MCI and 21 age-matched normal control subjects	Vessel density of retinal vascular network, superficial capillary plexus, and deep capillary plexus.	<ul style="list-style-type: none"> <li>• Decreased density of retinal vascular network, superficial vascular plexus, and deep vascular plexus in AD dementia (p&lt;0.05), compared with controls.</li> </ul>
Bulut et al. (2018) <sup>S67</sup>	26 AD dementia and 26 age-gender matched normal control subjects	Vessel density and foveal avascular zone area of superficial capillary plexus.	<ul style="list-style-type: none"> <li>• Decreased density (45.40% vs. 48.67%, p=0.002) and enlarged foveal avascular zone area (0.47mm<sup>2</sup> vs. 0.33mm<sup>2</sup>, p=0.001) of superficial capillary plexus in AD dementia, compared with controls.</li> </ul>
O'Bryhim et al. (2018) <sup>S74</sup>	14 preclinical AD (A $\beta$ -positive from PET or CSF but not dementia) and 16 normal control subjects	Foveal avascular zone area.	<ul style="list-style-type: none"> <li>• Enlarged foveal avascular zone area (0.364mm<sup>2</sup> vs. 0.275mm<sup>2</sup>, p=0.002) in preclinical AD, compared with controls, with AUROC of 0.8007.</li> </ul>
Lahme et al. (2018) <sup>S69</sup>	36 AD dementia and 27 normal control subjects	Foveal avascular zone area and vessel density of superficial capillary plexus, deep capillary plexus and radial peripapillary capillary.	<ul style="list-style-type: none"> <li>• Decreased vessel density of superficial capillary plexus (48.77% vs. 51.64%, p=0.001) and radial peripapillary capillary (53.07% vs. 55.39%, p=0.015) in AD dementia, compared with controls.</li> <li>• No significant correlation between A<math>\beta</math> or tau levels in the CSF and OCT-angiography measures.</li> </ul>
Querques et al. (2019) <sup>S71</sup>	12 AD dementia, 12 MCI, and 32 age-gender matched normal control subjects	Vessel density of superficial capillary plexus and deep capillary plexus	<ul style="list-style-type: none"> <li>• No differences in all the measures.</li> </ul>
den Haan et al. (2019) <sup>S72</sup>	48 AD dementia, and 38 normal control subjects	Vessel density and foveal avascular zone area	<ul style="list-style-type: none"> <li>• No differences in all the measures.</li> </ul>
Zhang et al. (2019) <sup>S70</sup>	16 early AD or amnesic MCI, and 16 normal control subjects	Vessel density and vessel length density of superficial capillary plexus, radial peripapillary capillary and peripapillary superficial vascular plexus. Adjusted	<ul style="list-style-type: none"> <li>• Decreased vessel density (40.67% vs. 44.5%, p=0.028) and adjusted flow index (0.376 vs. 0.407, p=0.047) of superficial capillary plexus in early AD or amnesic MCI, compared with controls.</li> </ul>

		flow index of superficial capillary plexus.	
van de Kreeke et al. (2019) <sup>S75</sup>	13 preclinical AD (A $\beta$ -positive from PET but not dementia) and 111 normal control subjects	Foveal avascular zone area and vessel density of retinal vascular network at inner ring macula and outer ring macula, and around optic nerve head.	<ul style="list-style-type: none"> <li>• Increased vessel density of retinal vascular network at inner ring macula (difference: 0.81%, p=0.002) and outer ring macula (difference: 0.50%, p=0.024), and around optic nerve head (difference: 0.83%, p=0.015) in preclinical AD, compared with controls.</li> <li>• AUROCs for vessel densities in inner and outer ring of the macula and around the optic nerve head were 0.651, 0.640 and 0.764,</li> </ul>
Zabel et al. (2019) <sup>S73</sup>	27 AD dementia, 27 open-angle glaucoma and 27 normal control subjects	Foveal avascular zone area and vessel density of superficial capillary plexus, deep capillary plexus and radial peripapillary capillary.	<ul style="list-style-type: none"> <li>• Decreased vessel density of deep capillary plexus (43.95% vs. 47.44% vs. 49.46%, p=0.0006) and enlarged foveal avascular zone area (0.32mm<sup>2</sup> vs. 0.26mm<sup>2</sup> vs. 0.21mm<sup>2</sup>, p&lt;0.001) in AD dementia, compared with open-angle glaucoma and controls.</li> </ul>
Lee et al. (2020) <sup>S201</sup>	29 AD-related cognitive impairment, 25 subcortical vascular cognitive impairment and 15 normal control subjects	Vessel density of radial peripapillary capillary.	<ul style="list-style-type: none"> <li>• No differences in vessel density of radial peripapillary capillary between AD-related cognitive impairment and normal control subjects.</li> </ul>
<b><u>OCT with EDI studies</u></b>			
Gharbiya et al. (2014) <sup>S80</sup>	21 mild to moderate AD dementia and 21 age-matched normal control subjects	Choroidal thickness	<ul style="list-style-type: none"> <li>• Reduced choroidal thicknesses in AD dementia (subfoveal choroidal thickness: 200.9<math>\mu</math>m vs. 266.1<math>\mu</math>m, p=0.001; other regions: p<math>\leq</math>0.036).</li> </ul>
Bayhan et al. (2015) <sup>S79</sup>	31 AD dementia and 30 age-matched normal control subjects	Choroidal thickness	<ul style="list-style-type: none"> <li>• Reduced choroidal (subfoveal choroidal thickness: 221.48<math>\mu</math>m vs. 251.86<math>\mu</math>m, p=0.001; other regions: all p<math>\leq</math>0.036, except measurement at 3.0 mm temporal to the fovea [p=0.067]) thickness in AD dementia.</li> </ul>
Trebbastoni et al. (2017) <sup>S81</sup>	39 AD dementia and 39 normal control subjects	Choroidal thickness	<ul style="list-style-type: none"> <li>• A larger reduction in choroidal thicknesses (changes in subfoveal choroidal thickness: -10.47<math>\mu</math>m vs. -2.0<math>\mu</math>m) in AD dementia over a 12-month follow-up, compared with controls.</li> </ul>
Bulut et al. (2018) <sup>S67</sup>	26 AD dementia and 26 age-gender matched normal control subjects	Choroidal thickness	<ul style="list-style-type: none"> <li>• Reduced choroidal thickness (198.27<math>\mu</math>m vs. 251.88<math>\mu</math>m, p&lt;0.001) in AD dementia, compared with controls.</li> </ul>

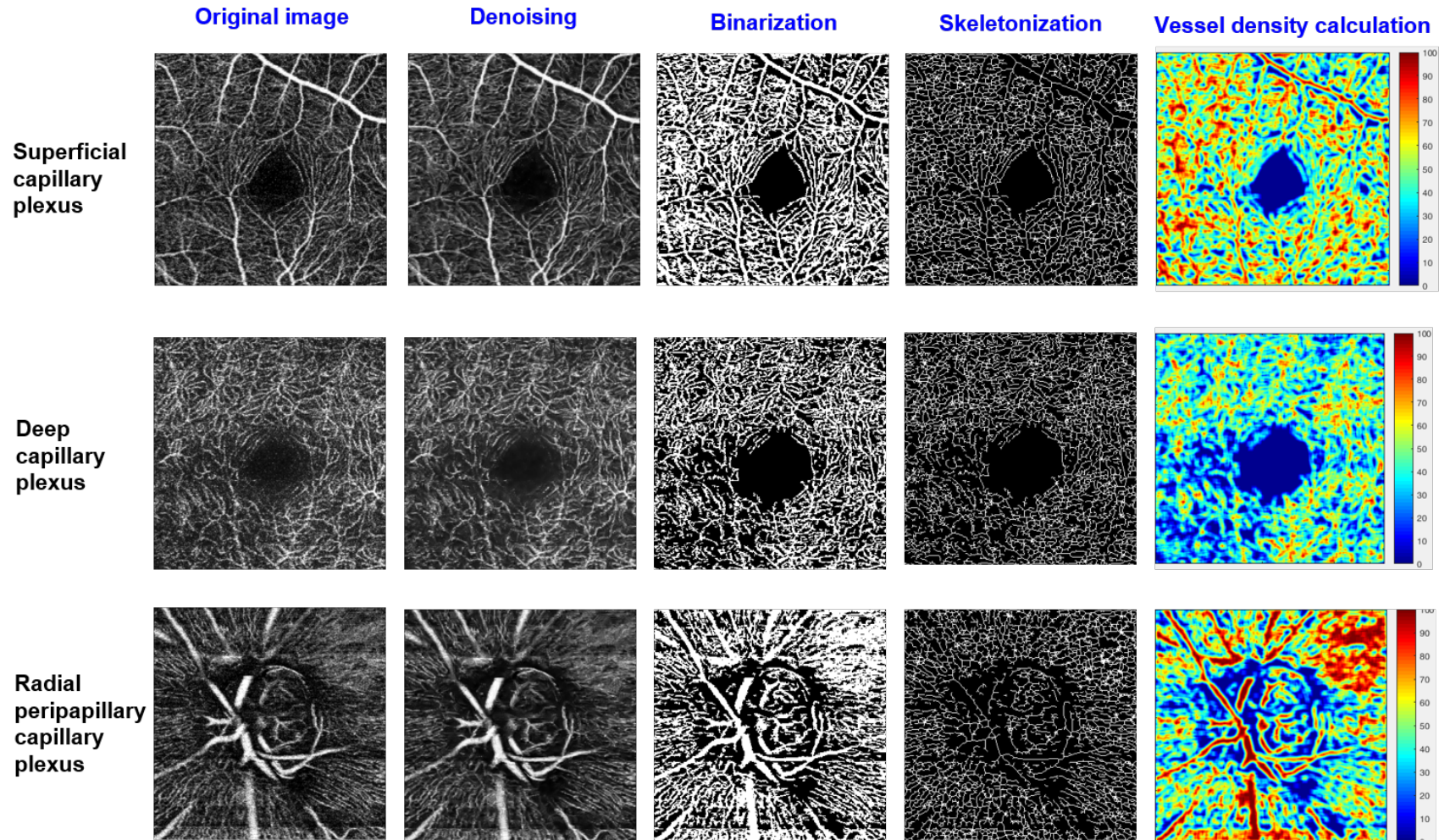
<b>Retinal photography studies</b>			
Frost et al. (2013) <sup>39</sup>	25 AD dementia, and 123 age-matched control subjects  Among control group, 15 A $\beta$ -positive (preclinical AD) and 30 A $\beta$ -negative subjects	CRAE, CRVE, FD, tortuosity, bifurcation	<ul style="list-style-type: none"> <li>• Decreased CRAE (122.9<math>\mu</math>m vs. 129.1<math>\mu</math>m, p=0.01), CRVE (169.7<math>\mu</math>m vs. 182.7<math>\mu</math>m, p&lt;0.001), arteriolar FD (1.201 vs. 1.235, p=0.008), venular FD (1.171 vs. 1.210, p&lt;0.001), venular tortuosity (6.953x10<sup>-5</sup> vs. 7.660x10<sup>-5</sup>, p=0.024) and venular branching coefficient (1.347 vs. 1.253, p=0.019) in AD dementia, compared with controls.</li> <li>• Increased venular branching asymmetry factor (p=0.01) and arteriolar length-to-diameter ratio (p=0.02) in preclinical AD, compared with A<math>\beta</math>-negative subjects.</li> </ul>
Cheung et al. (2014) <sup>40</sup>	136 AD dementia, and 290 age-matched control subjects	CRAE, CRVE, FD, tortuosity, bifurcation	<ul style="list-style-type: none"> <li>• Decreased CRVE (OR 2.01 [1.27, 3.19]), arteriolar (OR 1.35 [1.08, 1.68]) and venular (OR 1.47 [1.17, 1.84]) FDs, and increased arteriolar (OR 1.80 [1.40, 2.31]) and venular (OR 1.94 [1.48, 2.53]) tortuosity associated with AD dementia.</li> </ul>
Williams et al.(2015) <sup>41</sup>	213 AD dementia, and 294 age-matched control subjects	CRAE, CRVE, FD, tortuosity, bifurcation	<ul style="list-style-type: none"> <li>• Decreased total FD (OR 0.77 [0.62, 0.97]) and arteriolar tortuosity (OR 0.78 [0.63, 0.97]) associated with AD dementia.</li> </ul>
den Haan et al. (2019) <sup>S72</sup>	48 AD dementia, and 38 normal control subjects	CRAE, CRVE, FD, tortuosity	<ul style="list-style-type: none"> <li>• No differences in all the measures</li> </ul>

A $\beta$ =amyloid-beta; AD=Alzheimer's disease; AUROC=area under receiver operating characteristic curve; CRAE=central retinal artery equivalent; CRVE=central retinal vein equivalent; CSF=cerebrospinal fluid; EDI=enhanced depth imaging; FD=fractal dimension; GCC=ganglion cell complex; GC-IPL=ganglion cell-inner plexiform layer; GCL= ganglion cell layer; HR=hazard ratio; INL=inner nuclear layer; IPL=inner plexiform layer; MCI=mild cognitive impairment; OPL=outer plexiform layer; ONL=outer nuclear layer; OR=odds ratio; RNFL=retinal nerve fiber layer; RPE=retinal pigment epithelium; OCT=optical coherence tomography; PET=positron emission tomography.

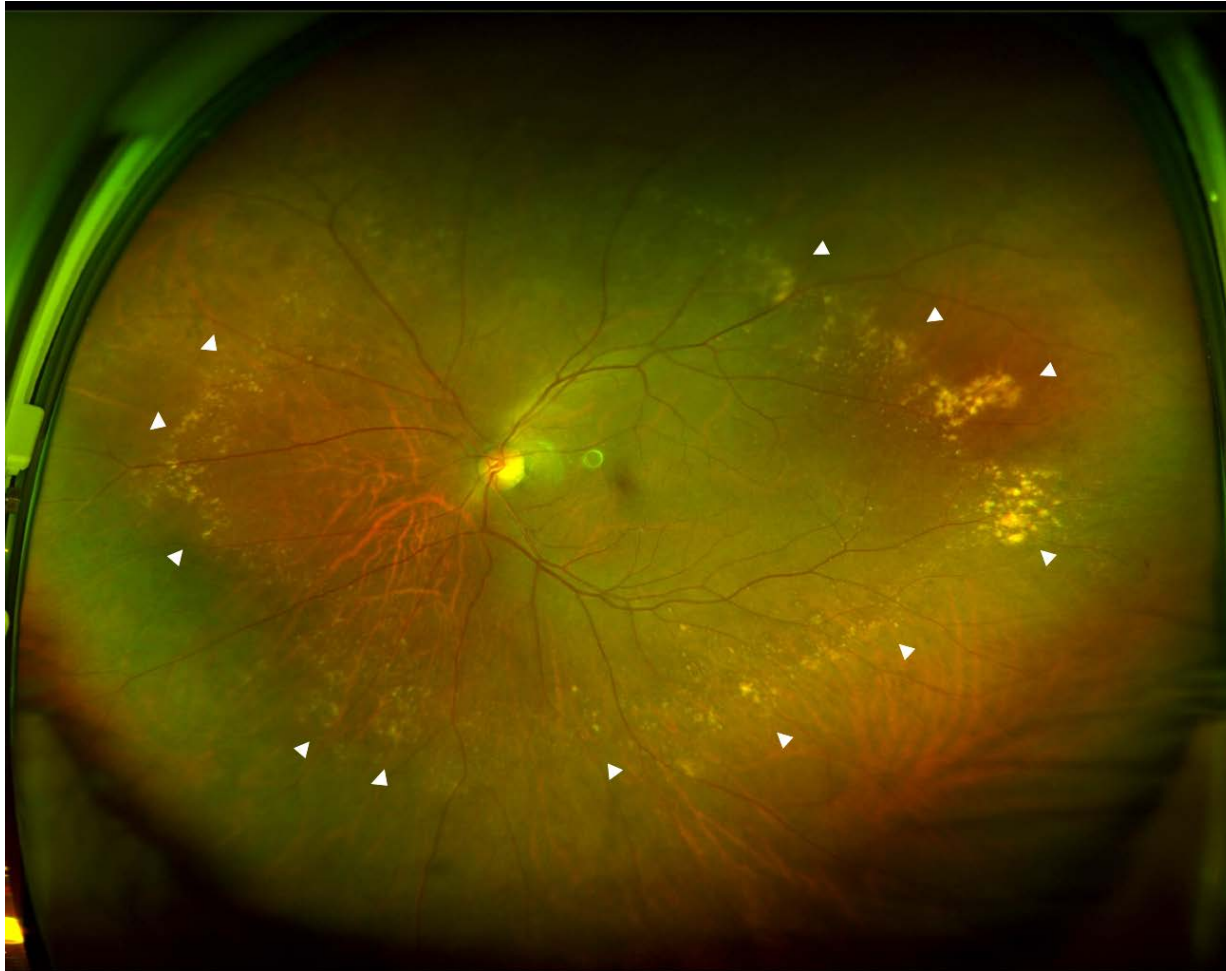
**Supplementary Table 3.** A proposed framework of research using retinal imaging technology as a source of biomarkers for Alzheimer’s disease (AD).

Items in the Framework	Examples
1. Study should be designed and conducted with a specific clinical purpose.	Can spectral-domain (SD-OCT) be used as a screening tool to identify asymptomatic individuals who are more likely to have AD in community, neurology clinics, eye clinics or optical shops?
2. Diagnosis of AD should be defined in a consistent manner with the latest available criteria.	AD should be defined by biomarkers of amyloid- $\beta$ deposition, pathologic tau, and neurodegeneration. <sup>8</sup>
3. Standard statistical measures of accuracy of biomarkers should be reported.	The sensitivity, specificity, false-positive and false-negative rates of SD-OCT measures should be reported, using the above as a reference standard.
4. Studies should be designed carefully to take into account many age-related ocular conditions.	How do different ocular conditions (e.g. glaucoma, age-related macular degeneration and elongated eyeball) manifest on SD-OCT? How do these ocular conditions be considered in the analysis and interpretation?
5. The reproducibility of the retinal imaging measures should be determined.	What are the intra-visit repeatability and inter-visit reproducibility of SD-OCT measures?
6. The incremental benefit and cost-effectiveness of retinal imaging as well as acceptability to patients in different settings should be evaluated.	What are the benefits to screen AD using SD-OCT in community, neurology clinics, eye clinics or optical shops?

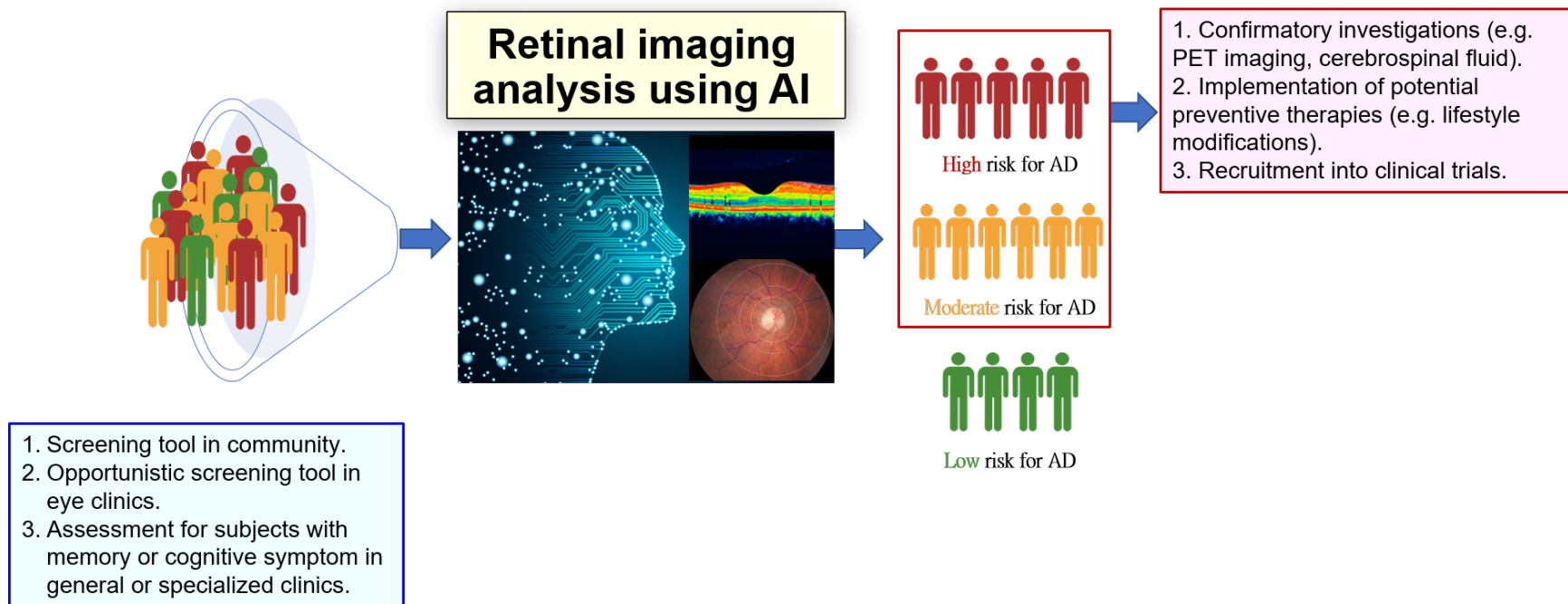
**Supplementary Figure 1.** Image processing steps (e.g. image denoising, binarization, skeletonization) to quantify the retinal capillary networks (superficial capillary plexus, deep capillary plexus and radial peripapillary capillary plexus) from optical coherence tomography angiography (OCT-A) images in a subject with Alzheimer disease dementia.



**Supplementary Figure 2.** An example of presence of drusen deposits in the peripheral retina (appear as yellow deposits under the retina, indicated by white arrows) imaged by ultra-widefield scanning laser ophthalmoscopy (Daytona, Optos, Dunfermline, UK) in a 77-year-old subject with Alzheimer's disease dementia (global clinical dementia rating score of 1). Except presence of drusen deposits in the peripheral retina, no other retinal disorders were observed in this subject. These peripheral drusen deposits are not present in healthy individuals without eye diseases.



**Supplementary Figure 3.** A proposed pathway of screening Alzheimer’s disease (AD) using retinal imaging assisted by artificial intelligence (AI). By providing a simple 2-tier risk stratification output, the AI algorithm could assist physicians to identify asymptomatic individuals who are more likely to have AD in different settings (e.g. community-based, eye clinic-based, general or specialized clinics). The high-risk group can then benefit from subsequent confirmatory investigations (e.g. PET imaging and cerebrospinal fluid tests), implementation of potential preventive therapies or recruitment into clinical trials.



## Supplementary References

- S1. Koronyo Y, Biggs D, Barron E, et al. Retinal amyloid pathology and proof-of-concept imaging trial in Alzheimer's disease. *JCI Insight* 2017;2(16) doi: 10.1172/jci.insight.93621
- S2. Keenan TD, Goldacre R, Goldacre MJ. Associations between age-related macular degeneration, Alzheimer disease, and dementia: record linkage study of hospital admissions. *JAMA Ophthalmol* 2014;132(1):63-8. doi: 10.1001/jamaophthalmol.2013.5696
- S3. Williams MA, Silvestri V, Craig D, et al. The prevalence of age-related macular degeneration in Alzheimer's disease. *J Alzheimers Dis* 2014;42(3):909-14. doi: 10.3233/JAD-140243
- S4. Tsai DC, Chen SJ, Huang CC, et al. Age-Related Macular Degeneration and Risk of Degenerative Dementia among the Elderly in Taiwan: A Population-Based Cohort Study. *Ophthalmology* 2015;122(11):2327-35 e2. doi: 10.1016/j.ophtha.2015.07.033
- S5. Lee CS, Larson EB, Gibbons LE, et al. Associations between recent and established ophthalmic conditions and risk of Alzheimer's disease. *Alzheimers Dement* 2019;15(1):34-41. doi: 10.1016/j.jalz.2018.06.2856
- S6. Lin IC, Wang YH, Wang TJ, et al. Glaucoma, Alzheimer's disease, and Parkinson's disease: an 8-year population-based follow-up study. *PLoS One* 2014;9(9):e108938. doi: 10.1371/journal.pone.0108938
- S7. Keenan TD, Goldacre R, Goldacre MJ. Associations between primary open angle glaucoma, Alzheimer's disease and vascular dementia: record linkage study. *Br J Ophthalmol* 2015;99(4):524-7. doi: 10.1136/bjophthalmol-2014-305863
- S8. Lin MY, Gutierrez PR, Stone KL, et al. Vision impairment and combined vision and hearing impairment predict cognitive and functional decline in older women. *J Am Geriatr Soc* 2004;52(12):1996-2002. doi: 10.1111/j.1532-5415.2004.52554.x
- S9. Reyes-Ortiz CA, Kuo YF, DiNuzzo AR, et al. Near vision impairment predicts cognitive decline: data from the Hispanic Established Populations for Epidemiologic Studies of the Elderly. *J Am Geriatr Soc* 2005;53(4):681-6. doi: 10.1111/j.1532-5415.2005.53219.x
- S10. Rogers MA, Langa KM. Untreated poor vision: a contributing factor to late-life dementia. *Am J Epidemiol* 2010;171(6):728-35. doi: 10.1093/aje/kwp453
- S11. Ong SY, Cheung CY, Li X, et al. Visual impairment, age-related eye diseases, and cognitive function: the Singapore Malay Eye study. *Arch Ophthalmol* 2012;130(7):895-900. doi: 10.1001/archophthalmol.2012.152

- S12. Hajek A, Brettschneider C, Luhmann D, et al. Effect of Visual Impairment on Physical and Cognitive Function in Old Age: Findings of a Population-Based Prospective Cohort Study in Germany. *J Am Geriatr Soc* 2016;64(11):2311-16. doi: 10.1111/jgs.14458
- S13. Chen SP, Bhattacharya J, Pershing S. Association of Vision Loss With Cognition in Older Adults. *JAMA Ophthalmol* 2017;135(9):963-70. doi: 10.1001/jamaophthalmol.2017.2838
- S14. Maharani A, Dawes P, Nazroo J, et al. Visual and hearing impairments are associated with cognitive decline in older people. *Age Ageing* 2018;47(4):575-81. doi: 10.1093/ageing/afy061
- S15. Clemons TE, Rankin MW, McBee WL, et al. Cognitive impairment in the Age-Related Eye Disease Study: AREDS report no. 16. *Arch Ophthalmol* 2006;124(4):537-43. doi: 10.1001/archophth.124.4.537
- S16. Woo SJ, Park KH, Ahn J, et al. Cognitive impairment in age-related macular degeneration and geographic atrophy. *Ophthalmology* 2012;119(10):2094-101. doi: 10.1016/j.ophtha.2012.04.026
- S17. Pham TQ, Kifley A, Mitchell P, et al. Relation of age-related macular degeneration and cognitive impairment in an older population. *Gerontology* 2006;52(6):353-8. doi: 10.1159/000094984
- S18. Baker ML, Wang JJ, Rogers S, et al. Early age-related macular degeneration, cognitive function, and dementia: the Cardiovascular Health Study. *Arch Ophthalmol* 2009;127(5):667-73. doi: 10.1001/archophthalmol.2009.30
- S19. Wong TY, Klein R, Nieto FJ, et al. Is early age-related maculopathy related to cognitive function? The Atherosclerosis Risk in Communities Study. *Am J Ophthalmol* 2002;134(6):828-35.
- S20. Blanks JC, Hinton DR, Sadun AA, et al. Retinal ganglion cell degeneration in Alzheimer's disease. *Brain Res* 1989;501(2):364-72.
- S21. Hinton DR, Sadun AA, Blanks JC, et al. Optic-nerve degeneration in Alzheimer's disease. *N Engl J Med* 1986;315(8):485-7. doi: 10.1056/NEJM198608213150804
- S22. Parisi V, Restuccia R, Fattapposta F, et al. Morphological and functional retinal impairment in Alzheimer's disease patients. *Clin Neurophysiol* 2001;112(10):1860-7.
- S23. Iseri PK, Altinas O, Tokay T, et al. Relationship between cognitive impairment and retinal morphological and visual functional abnormalities in Alzheimer disease. *J Neuroophthalmol* 2006;26(1):18-24. doi: 10.1097/01.wno.0000204645.56873.26

- S24. Paquet C, Boissonnot M, Roger F, et al. Abnormal retinal thickness in patients with mild cognitive impairment and Alzheimer's disease. *Neurosci Lett* 2007;420(2):97-9. doi: 10.1016/j.neulet.2007.02.090
- S25. Lu Y, Li Z, Zhang X, et al. Retinal nerve fiber layer structure abnormalities in early Alzheimer's disease: evidence in optical coherence tomography. *Neurosci Lett* 2010;480(1):69-72. doi: 10.1016/j.neulet.2010.06.006
- S26. Kesler A, Vakhapova V, Korczyn AD, et al. Retinal thickness in patients with mild cognitive impairment and Alzheimer's disease. *Clin Neurol Neurosurg* 2011;113(7):523-6. doi: 10.1016/j.clineuro.2011.02.014
- S27. Berisha F, Fekete GT, Trempe CL, et al. Retinal abnormalities in early Alzheimer's disease. *Invest Ophthalmol VisSci* 2007;48(5):2285-89.
- S28. Paquet C, Boissonnot M, Roger F, et al. Abnormal retinal thickness in patients with mild cognitive impairment and Alzheimer's disease. *NeurosciLett* 2007;420(2):97-99.
- S29. Moschos MM, Markopoulos I, Chatziralli I, et al. Structural and functional impairment of the retina and optic nerve in Alzheimer's disease. *Curr Alzheimer Res* 2012;9(7):782-8.
- S30. Garcia-Martin ES, Rojas B, Ramirez AI, et al. Macular thickness as a potential biomarker of mild Alzheimer's disease. *Ophthalmology* 2014;121(5):1149-51 e3. doi: 10.1016/j.ophtha.2013.12.023
- S31. Garcia-Martin E, Satue M, Fuertes I, et al. Ability and reproducibility of Fourier-domain optical coherence tomography to detect retinal nerve fiber layer atrophy in Parkinson's disease. *Ophthalmology* 2012;119(10):2161-7. doi: 10.1016/j.ophtha.2012.05.003
- S32. Ascaso FJ, Cruz N, Modrego PJ, et al. Retinal alterations in mild cognitive impairment and Alzheimer's disease: an optical coherence tomography study. *J Neurol* 2014;261(8):1522-30. doi: 10.1007/s00415-014-7374-z
- S33. Danesh-Meyer HV, Birch H, Ku JY, et al. Reduction of optic nerve fibers in patients with Alzheimer disease identified by laser imaging. *Neurology* 2006;67(10):1852-4. doi: 10.1212/01.wnl.0000244490.07925.8b [published Online First: 2006/11/30]
- S34. Kergoat H, Kergoat MJ, Justino L, et al. An evaluation of the retinal nerve fiber layer thickness by scanning laser polarimetry in individuals with dementia of the Alzheimer type. *Acta Ophthalmol Scand* 2001;79(2):187-91. [published Online First: 2001/04/04]
- S35. Drexler W, Fujimoto JG. State-of-the-art retinal optical coherence tomography. *Prog Retin Eye Res* 2008;27(1):45-88. doi: 10.1016/j.preteyeres.2007.07.005
- S36. Curcio CA, Allen KA. Topography of ganglion cells in human retina. *J Comp Neurol* 1990;300(1):5-25. doi: 10.1002/cne.903000103

- S37. Loh EH, Ong YT, Venketasubramanian N, et al. Repeatability and Reproducibility of Retinal Neuronal and Axonal Measures on Spectral-Domain Optical Coherence Tomography in Patients with Cognitive Impairment. *Front Neurol* 2017;8:359. doi: 10.3389/fneur.2017.00359
- S38. Lad EM, Mukherjee D, Stinnett SS, et al. Evaluation of inner retinal layers as biomarkers in mild cognitive impairment to moderate Alzheimer's disease. *PLoS One* 2018;13(2):e0192646. doi: 10.1371/journal.pone.0192646
- S39. Snyder PJ, Johnson LN, Lim YY, et al. Nonvascular retinal imaging markers of preclinical Alzheimer's disease. *Alzheimers Dement (Amst)* 2016;4:169-78. doi: 10.1016/j.dadm.2016.09.001
- S40. Moreno-Ramos T, Benito-Leon J, Villarejo A, et al. Retinal nerve fiber layer thinning in dementia associated with Parkinson's disease, dementia with Lewy bodies, and Alzheimer's disease. *J Alzheimers Dis* 2013;34(3):659-64. doi: 10.3233/JAD-121975
- S41. Unlu M, Gulmez Sevim D, Gultekin M, et al. Correlations among multifocal electroretinography and optical coherence tomography findings in patients with Parkinson's disease. *Neurol Sci* 2018;39(3):533-41. doi: 10.1007/s10072-018-3244-2
- S42. den Haan J, Csinscik L, Parker T, et al. Retinal thickness as potential biomarker in posterior cortical atrophy and typical Alzheimer's disease. *Alzheimers Res Ther* 2019;11(1):62. doi: 10.1186/s13195-019-0516-x
- S43. Ning A, Cui J, To E, et al. Amyloid-beta deposits lead to retinal degeneration in a mouse model of Alzheimer disease. *Invest Ophthalmol Vis Sci* 2008;49(11):5136-43. doi: 10.1167/iovs.08-1849
- S44. Koronyo-Hamaoui M, Koronyo Y, Ljubimov AV, et al. Identification of amyloid plaques in retinas from Alzheimer's patients and noninvasive in vivo optical imaging of retinal plaques in a mouse model. *Neuroimage* 2011;54 Suppl 1:S204-17. doi: 10.1016/j.neuroimage.2010.06.020
- S45. Schon C, Hoffmann NA, Ochs SM, et al. Long-term in vivo imaging of fibrillar tau in the retina of P301S transgenic mice. *PLoS One* 2012;7(12):e53547. doi: 10.1371/journal.pone.0053547
- S46. Liu B, Rasool S, Yang Z, et al. Amyloid-peptide vaccinations reduce {beta}-amyloid plaques but exacerbate vascular deposition and inflammation in the retina of Alzheimer's transgenic mice. *Am J Pathol* 2009;175(5):2099-110. doi: 10.2353/ajpath.2009.090159
- S47. Perez SE, Lumayag S, Kovacs B, et al. Beta-amyloid deposition and functional impairment in the retina of the APP<sup>swe</sup>/PS1<sup>DeltaE9</sup> transgenic mouse model of Alzheimer's disease. *Invest Ophthalmol Vis Sci* 2009;50(2):793-800. doi: 10.1167/iovs.08-2384

- S48. Zhang YS, Onishi AC, Zhou N, et al. Characterization of Inner Retinal Hyperreflective Alterations in Early Cognitive Impairment on Adaptive Optics Scanning Laser Ophthalmoscopy. *Invest Ophthalmol Vis Sci* 2019;60(10):3527-36. doi: 10.1167/iovs.19-27135
- S49. De Silva TM, Faraci FM. Microvascular Dysfunction and Cognitive Impairment. *Cell Mol Neurobiol* 2016;36(2):241-58. doi: 10.1007/s10571-015-0308-1
- S50. Wardlaw JM, Smith EE, Biessels GJ, et al. Neuroimaging standards for research into small vessel disease and its contribution to ageing and neurodegeneration. *Lancet Neurol* 2013;12(8):822-38. doi: 10.1016/S1474-4422(13)70124-8
- S51. van Veluw SJ, Hilal S, Kuijf HJ, et al. Cortical microinfarcts on 3T MRI: Clinical correlates in memory-clinic patients. *Alzheimers Dement* 2015;11(12):1500-9. doi: 10.1016/j.jalz.2014.12.010
- S52. Arvanitakis Z, Capuano AW, Leurgans SE, et al. Relation of cerebral vessel disease to Alzheimer's disease dementia and cognitive function in elderly people: a cross-sectional study. *Lancet Neurol* 2016;15(9):934-43. doi: 10.1016/S1474-4422(16)30029-1
- S53. Murray CD. The Physiological Principle of Minimum Work: I. The Vascular System and the Cost of Blood Volume. *Proc Natl Acad Sci USA* 1926;12(3):207-14.
- S54. Cheung CY, Lamoureux E, Ikram MK, et al. Retinal vascular geometry in Asian persons with diabetes and retinopathy. *J Diabetes Sci Technol* 2012;6(3):595-605. doi: 10.1177/193229681200600315
- S55. Cheung CY, Tay WT, Mitchell P, et al. Quantitative and qualitative retinal microvascular characteristics and blood pressure. *J Hypertens* 2011;29(7):1380-91. doi: 10.1097/HJH.0b013e328347266c
- S56. Witt N, Wong TY, Hughes AD, et al. Abnormalities of retinal microvascular structure and risk of mortality from ischemic heart disease and stroke. *Hypertension* 2006;47(5):975-81.
- S57. McGrory S, Taylor AM, Pellegrini E, et al. Towards Standardization of Quantitative Retinal Vascular Parameters: Comparison of SIVA and VAMPIRE Measurements in the Lothian Birth Cohort 1936. *Transl Vis Sci Technol* 2018;7(2):12. doi: 10.1167/tvst.7.2.12
- S58. Welikala RA, Fraz MM, Foster PJ, et al. Automated retinal image quality assessment on the UK Biobank dataset for epidemiological studies. *Comput Biol Med* 2016;71:67-76. doi: 10.1016/j.combiomed.2016.01.027
- S59. Tapp RJ, Owen CG, Barman SA, et al. Associations of Retinal Microvascular Diameters and Tortuosity With Blood Pressure and Arterial Stiffness: United Kingdom Biobank. *Hypertension* 2019;74(6):1383-90. doi: 10.1161/HYPERTENSIONAHA.119.13752

- S60. Thomas GN, Ong SY, Tham YC, et al. Measurement of macular fractal dimension using a computer-assisted program. *Invest Ophthalmol Vis Sci* 2014;55(4):2237-43. doi: 10.1167/iovs.13-13315
- S61. Perez-Rovira A, MacGillivray T, Trucco E, et al. VAMPIRE: Vessel assessment and measurement platform for images of the REtina. *Conf Proc IEEE Eng Med Biol Soc* 2011;2011:3391-4. doi: 10.1109/IEMBS.2011.6090918
- S62. Sasongko MB, Wong TY, Nguyen TT, et al. Retinal vascular tortuosity in persons with diabetes and diabetic retinopathy. *Diabetologia* 2011;54(9):2409-16. doi: 10.1007/s00125-011-2200-y
- S63. Tang FY, Ng DS, Lam A, et al. Determinants of Quantitative Optical Coherence Tomography Angiography Metrics in Patients with Diabetes. *Sci Rep* 2017;7(1):2575. doi: 10.1038/s41598-017-02767-0
- S64. Jia Y, Bailey ST, Hwang TS, et al. Quantitative optical coherence tomography angiography of vascular abnormalities in the living human eye. *Proc Natl Acad Sci U S A* 2015;112(18):E2395-402. doi: 10.1073/pnas.1500185112
- S65. Spaide RF, Fujimoto JG, Waheed NK, et al. Optical coherence tomography angiography. *Prog Retin Eye Res* 2018;64:1-55. doi: 10.1016/j.preteyeres.2017.11.003
- S66. Sun Z, Tang F, Wong R, et al. OCT Angiography Metrics Predict Progression of Diabetic Retinopathy and Development of Diabetic Macular Edema: A Prospective Study. *Ophthalmology* 2019;126(12):1675-84. doi: 10.1016/j.ophtha.2019.06.016
- S67. Bulut M, Kurtulus F, Gozkaya O, et al. Evaluation of optical coherence tomography angiographic findings in Alzheimer's type dementia. *Br J Ophthalmol* 2018;102(2):233-37. doi: 10.1136/bjophthalmol-2017-310476
- S68. Jiang H, Wei Y, Shi Y, et al. Altered Macular Microvasculature in Mild Cognitive Impairment and Alzheimer Disease. *J Neuroophthalmol* 2018;38(3):292-98. doi: 10.1097/WNO.0000000000000580
- S69. Lahme L, Esser EL, Mihailovic N, et al. Evaluation of Ocular Perfusion in Alzheimer's Disease Using Optical Coherence Tomography Angiography. *J Alzheimers Dis* 2018;66(4):1745-52. doi: 10.3233/JAD-180738
- S70. Zhang YS, Zhou N, Knoll BM, et al. Parafoveal vessel loss and correlation between peripapillary vessel density and cognitive performance in amnesic mild cognitive impairment and early Alzheimer's Disease on optical coherence tomography angiography. *PLoS One* 2019;14(4):e0214685. doi: 10.1371/journal.pone.0214685

- S71. Querques G, Borrelli E, Sacconi R, et al. Functional and morphological changes of the retinal vessels in Alzheimer's disease and mild cognitive impairment. *Sci Rep* 2019;9(1):63. doi: 10.1038/s41598-018-37271-6
- S72. Haan JD, van de Kreeke JA, van Berckel BN, et al. Is retinal vasculature a biomarker in amyloid proven Alzheimer's disease? *Alzheimers Dement (Amst)* 2019;11:383-91. doi: 10.1016/j.dadm.2019.03.006
- S73. Zabel P, Kaluzny JJ, Wilkosc-Debczynska M, et al. Comparison of Retinal Microvasculature in Patients With Alzheimer's Disease and Primary Open-Angle Glaucoma by Optical Coherence Tomography Angiography. *Invest Ophthalmol Vis Sci* 2019;60(10):3447-55. doi: 10.1167/iovs.19-27028
- S74. O'Bryhim BE, Apte RS, Kung N, et al. Association of Preclinical Alzheimer Disease With Optical Coherence Tomographic Angiography Findings. *JAMA Ophthalmol* 2018;136(11):1242-48. doi: 10.1001/jamaophthalmol.2018.3556
- S75. van de Kreeke JA, Nguyen HT, Konijnenberg E, et al. Optical coherence tomography angiography in preclinical Alzheimer's disease. *Br J Ophthalmol* 2020;104(2):157-61. doi: 10.1136/bjophthalmol-2019-314127
- S76. Bell RD, Winkler EA, Singh I, et al. Apolipoprotein E controls cerebrovascular integrity via cyclophilin A. *Nature* 2012;485(7399):512-6. doi: 10.1038/nature11087
- S77. Bell RD, Winkler EA, Sagare AP, et al. Pericytes control key neurovascular functions and neuronal phenotype in the adult brain and during brain aging. *Neuron* 2010;68(3):409-27. doi: 10.1016/j.neuron.2010.09.043
- S78. Bouras C, Kovari E, Herrmann FR, et al. Stereologic analysis of microvascular morphology in the elderly: Alzheimer disease pathology and cognitive status. *J Neuropathol Exp Neurol* 2006;65(3):235-44. doi: 10.1097/01.jnen.0000203077.53080.2c
- S79. Bayhan HA, Aslan Bayhan S, Celikbilek A, et al. Evaluation of the chorioretinal thickness changes in Alzheimer's disease using spectral-domain optical coherence tomography. *Clin Experiment Ophthalmol* 2015;43(2):145-51. doi: 10.1111/ceo.12386
- S80. Gharbiya M, Trebbastoni A, Parisi F, et al. Choroidal thinning as a new finding in Alzheimer's disease: evidence from enhanced depth imaging spectral domain optical coherence tomography. *J Alzheimers Dis* 2014;40(4):907-17. doi: 10.3233/JAD-132039
- S81. Trebbastoni A, Marcelli M, Mallone F, et al. Attenuation of Choroidal Thickness in Patients With Alzheimer Disease: Evidence From an Italian Prospective Study. *Alzheimer Dis Assoc Disord* 2017;31(2):128-34. doi: 10.1097/WAD.000000000000176
- S82. Tsai Y, Lu B, Ljubimov AV, et al. Ocular changes in TgF344-AD rat model of Alzheimer's disease. *Invest Ophthalmol Vis Sci* 2014;55(1):523-34. doi: 10.1167/iovs.13-12888

- S83. Jonas JB, Wang YX, Wei WB, et al. Cognitive Function and Subfoveal Choroidal Thickness: The Beijing Eye Study. *Ophthalmology* 2016;123(1):220-2. doi: 10.1016/j.ophtha.2015.06.020
- S84. Lim M, Sasongko MB, Ikram MK, et al. Systemic associations of dynamic retinal vessel analysis: a review of current literature. *Microcirculation* 2013;20(3):257-68. doi: 10.1111/micc.12026
- S85. Nguyen TT, Kawasaki R, Wang JJ, et al. Flicker light-induced retinal vasodilation in diabetes and diabetic retinopathy. *Diabetes Care* 2009;32(11):2075-80. doi: 10.2337/dc09-0075
- S86. Lim LS, Ling LH, Ong PG, et al. Dynamic responses in retinal vessel caliber with flicker light stimulation in eyes with diabetic retinopathy. *Invest Ophthalmol Vis Sci* 2014;55(8):5207-13. doi: 10.1167/iovs.14-14301
- S87. Stefansson E, Olafsdottir OB, Eliasdottir TS, et al. Retinal oximetry: Metabolic imaging for diseases of the retina and brain. *Prog Retin Eye Res* 2019;70:1-22. doi: 10.1016/j.preteyeres.2019.04.001
- S88. Einarisdottir AB, Hardarson SH, Kristjansdottir JV, et al. Retinal oximetry imaging in Alzheimer's disease. *J Alzheimers Dis* 2016;49(1):79-83. doi: 10.3233/JAD-150457
- S89. Olafsdottir OB, Saevarsdottir HS, Hardarson SH, et al. Retinal oxygen metabolism in patients with mild cognitive impairment. *Alzheimers Dement (Amst)* 2018;10:340-45. doi: 10.1016/j.dadm.2018.03.002
- S90. Anderson DH, Talaga KC, Rivest AJ, et al. Characterization of beta amyloid assemblies in drusen: the deposits associated with aging and age-related macular degeneration. *Exp Eye Res* 2004;78(2):243-56.
- S91. Boyle PA, Yu L, Nag S, et al. Cerebral amyloid angiopathy and cognitive outcomes in community-based older persons. *Neurology* 2015;85(22):1930-6. doi: 10.1212/WNL.0000000000002175
- S92. Ukalovic K, Cao S, Lee S, et al. Drusen in the Peripheral Retina of the Alzheimer's Eye. *Curr Alzheimer Res* 2018;15(8):743-50. doi: 10.2174/1567205015666180123122637
- S93. Seddon JM, Reynolds R, Rosner B. Peripheral retinal drusen and reticular pigment: association with CFHY402H and CFHrs1410996 genotypes in family and twin studies. *Invest Ophthalmol Vis Sci* 2009;50(2):586-91. doi: 10.1167/iovs.08-2514
- S94. Dysli C, Wolf S, Berezin MY, et al. Fluorescence lifetime imaging ophthalmoscopy. *Prog Retin Eye Res* 2017;60:120-43. doi: 10.1016/j.preteyeres.2017.06.005

- S95. Jentsch S, Schweitzer D, Schmidtke KU, et al. Retinal fluorescence lifetime imaging ophthalmoscopy measures depend on the severity of Alzheimer's disease. *Acta Ophthalmol* 2015;93(4):e241-7. doi: 10.1111/aos.12609
- S96. Sadda SR, Borrelli E, Fan W, et al. A pilot study of fluorescence lifetime imaging ophthalmoscopy in preclinical Alzheimer's disease. *Eye (Lond)* 2019 doi: 10.1038/s41433-019-0406-2
- S97. Sung KR, Wollstein G, Bilonick RA, et al. Effects of age on optical coherence tomography measurements of healthy retinal nerve fiber layer, macula, and optic nerve head. *Ophthalmology* 2009;116(6):1119-24. doi: 10.1016/j.ophtha.2009.01.004 [published Online First: 2009/04/21]
- S98. Cheung CY, Chen D, Wong TY, et al. Determinants of quantitative optic nerve measurements using spectral domain optical coherence tomography in a population-based sample of non-glaucomatous subjects. *Invest Ophthalmol Vis Sci* 2011;52(13):9629-35. doi: 10.1167/iovs.11-7481
- S99. Koh VT, Tham YC, Cheung CY, et al. Determinants of ganglion cell-inner plexiform layer thickness measured by high-definition optical coherence tomography. *Invest Ophthalmol Vis Sci* 2012;53(9):5853-9. doi: 10.1167/iovs.12-10414
- S100. Leung CK, Yu M, Weinreb RN, et al. Retinal nerve fiber layer imaging with spectral-domain optical coherence tomography: a prospective analysis of age-related loss. *Ophthalmology* 2012;119(4):731-7. doi: 10.1016/j.ophtha.2011.10.010
- S101. Wong TY, Islam FM, Klein R, et al. Retinal vascular caliber, cardiovascular risk factors, and inflammation: the multi-ethnic study of atherosclerosis (MESA). *Invest Ophthalmol VisSci* 2006;47(6):2341-50.
- S102. Cheung CY, Zheng Y, Hsu W, et al. Retinal vascular tortuosity, blood pressure, and cardiovascular risk factors. *Ophthalmology* 2011;118(5):812-8. doi: 10.1016/j.ophtha.2010.08.045
- S103. Cheung CY, Thomas GN, Tay W, et al. Retinal vascular fractal dimension and its relationship with cardiovascular and ocular risk factors. *Am J Ophthalmol* 2012;154(4):663-74 e1. doi: 10.1016/j.ajo.2012.04.016
- S104. Gupta P, Jing T, Marziliano P, et al. Distribution and determinants of choroidal thickness and volume using automated segmentation software in a population-based study. *Am J Ophthalmol* 2015;159(2):293-301 e3. doi: 10.1016/j.ajo.2014.10.034
- S105. Myers CE, Klein R, Knudtson MD, et al. Determinants of retinal venular diameter: the Beaver Dam Eye Study. *Ophthalmology* 2012;119(12):2563-71. doi: 10.1016/j.ophtha.2012.06.038 [published Online First: 2012/08/25]

- S106. Gupta VK, Chitranshi N, Gupta VB, et al. Amyloid beta accumulation and inner retinal degenerative changes in Alzheimer's disease transgenic mouse. *Neurosci Lett* 2016;623:52-6. doi: 10.1016/j.neulet.2016.04.059
- S107. Cao L, Wang H, Wang F, et al. Aβ-induced senescent retinal pigment epithelial cells create a proinflammatory microenvironment in AMD. *Invest Ophthalmol Vis Sci* 2013;54(5):3738-50. doi: 10.1167/iovs.13-11612
- S108. Tsuruma K, Tanaka Y, Shimazawa M, et al. Induction of amyloid precursor protein by the neurotoxic peptide, amyloid-beta 25-35, causes retinal ganglion cell death. *J Neurochem* 2010;113(6):1545-54. doi: 10.1111/j.1471-4159.2010.06724.x
- S109. Guo L, Salt TE, Luong V, et al. Targeting amyloid-beta in glaucoma treatment. *Proc Natl Acad Sci U S A* 2007;104(33):13444-9. doi: 10.1073/pnas.0703707104
- S110. Ding JD, Johnson LV, Herrmann R, et al. Anti-amyloid therapy protects against retinal pigmented epithelium damage and vision loss in a model of age-related macular degeneration. *Proc Natl Acad Sci U S A* 2011;108(28):E279-87. doi: 10.1073/pnas.1100901108
- S111. Gasparini L, Crowther RA, Martin KR, et al. Tau inclusions in retinal ganglion cells of human P301S tau transgenic mice: effects on axonal viability. *Neurobiol Aging* 2011;32(3):419-33. doi: 10.1016/j.neurobiolaging.2009.03.002
- S112. Mazzaro N, Barini E, Spillantini MG, et al. Tau-Driven Neuronal and Neurotrophic Dysfunction in a Mouse Model of Early Tauopathy. *J Neurosci* 2016;36(7):2086-100. doi: 10.1523/JNEUROSCI.0774-15.2016
- S113. Shah TM, Gupta SM, Chatterjee P, et al. Beta-amyloid sequelae in the eye: a critical review on its diagnostic significance and clinical relevance in Alzheimer's disease. *Mol Psychiatry* 2017;22(3):353-63. doi: 10.1038/mp.2016.251
- S114. Williams EA, McGuone D, Frosch MP, et al. Absence of Alzheimer Disease Neuropathologic Changes in Eyes of Subjects With Alzheimer Disease. *J Neuropathol Exp Neurol* 2017;76(5):376-83. doi: 10.1093/jnen/nlx020
- S115. Ho CY, Troncoso JC, Knox D, et al. Beta-amyloid, phospho-tau and alpha-synuclein deposits similar to those in the brain are not identified in the eyes of Alzheimer's and Parkinson's disease patients. *Brain Pathol* 2014;24(1):25-32. doi: 10.1111/bpa.12070
- S116. den Haan J, Morrema THJ, Verbraak FD, et al. Amyloid-beta and phosphorylated tau in post-mortem Alzheimer's disease retinas. *Acta Neuropathol Commun* 2018;6(1):147. doi: 10.1186/s40478-018-0650-x

- S117. DeTure MA, Dickson DW. The neuropathological diagnosis of Alzheimer's disease. *Mol Neurodegener* 2019;14(1):32. doi: 10.1186/s13024-019-0333-5 [published Online First: 2019/08/04]
- S118. Leung CK, Cheung CY, Weinreb RN, et al. Retinal nerve fiber layer imaging with spectral-domain optical coherence tomography: a variability and diagnostic performance study. *Ophthalmology* 2009;116(7):1257-63, 63 e1-2. doi: 10.1016/j.ophtha.2009.04.013
- S119. Harvey AR, Carles G, Bradu A, et al. Chapter 3 - The physics, instruments and modalities of retinal imaging. In: Trucco E, MacGillivray T, Xu Y, eds. *Computational Retinal Image Analysis*: Academic Press 2019:19-57.
- S120. More SS, Beach JM, Vince R. Early Detection of Amyloidopathy in Alzheimer's Mice by Hyperspectral Endoscopy. *Invest Ophthalmol Vis Sci* 2016;57(7):3231-8. doi: 10.1167/iovs.15-17406
- S121. More SS, Vince R. Hyperspectral imaging signatures detect amyloidopathy in Alzheimer's mouse retina well before onset of cognitive decline. *ACS Chem Neurosci* 2015;6(2):306-15. doi: 10.1021/cn500242z
- S122. More SS, Beach JM, McClelland C, et al. In Vivo Assessment of Retinal Biomarkers by Hyperspectral Imaging: Early Detection of Alzheimer's Disease. *ACS Chem Neurosci* 2019;10(11):4492-501. doi: 10.1021/acchemneuro.9b00331
- S123. Hadoux X, Hui F, Lim JKH, et al. Non-invasive in vivo hyperspectral imaging of the retina for potential biomarker use in Alzheimer's disease. *Nat Commun* 2019;10(1):4227. doi: 10.1038/s41467-019-12242-1
- S124. Sharafi SM, Sylvestre JP, Chevrefils C, et al. Vascular retinal biomarkers improves the detection of the likely cerebral amyloid status from hyperspectral retinal images. *Alzheimers Dement (N Y)* 2019;5:610-17. doi: 10.1016/j.trci.2019.09.006
- S125. Martinez B, Leon R, Fabelo H, et al. Most Relevant Spectral Bands Identification for Brain Cancer Detection Using Hyperspectral Imaging. *Sensors (Basel)* 2019;19(24) doi: 10.3390/s19245481
- S126. Giannoni L, Lange F, Tachtsidis I. Hyperspectral imaging solutions for brain tissue metabolic and hemodynamic monitoring: past, current and future developments. *J Opt* 2018;20(4):044009. doi: 10.1088/2040-8986/aab3a6
- S127. Lombardo M, Serrao S, Devaney N, et al. Adaptive optics technology for high-resolution retinal imaging. *Sensors (Basel)* 2013;13(1):334-66. doi: 10.3390/s130100334
- S128. Blanks JC, Schmidt SY, Torigoe Y, et al. Retinal pathology in Alzheimer's disease. II. Regional neuron loss and glial changes in GCL. *Neurobiol Aging* 1996;17(3):385-95. doi: 10.1016/0197-4580(96)00009-7

- S129. Ramirez AI, de Hoz R, Salobrar-Garcia E, et al. The Role of Microglia in Retinal Neurodegeneration: Alzheimer's Disease, Parkinson, and Glaucoma. *Front Aging Neurosci* 2017;9:214. doi: 10.3389/fnagi.2017.00214
- S130. Hinton G. Deep Learning-A Technology With the Potential to Transform Health Care. *JAMA* 2018;320(11):1101-02. doi: 10.1001/jama.2018.11100
- S131. Lancet T. Artificial intelligence in health care: within touching distance. *Lancet* 2018;390(10114):2739. doi: 10.1016/S0140-6736(17)31540-4
- S132. Ting DSW, Cheung CY, Lim G, et al. Development and Validation of a Deep Learning System for Diabetic Retinopathy and Related Eye Diseases Using Retinal Images From Multiethnic Populations With Diabetes. *JAMA* 2017;318(22):2211-23. doi: 10.1001/jama.2017.18152
- S133. Abramoff MD, Lou Y, Erginay A, et al. Improved Automated Detection of Diabetic Retinopathy on a Publicly Available Dataset Through Integration of Deep Learning. *Invest Ophthalmol Vis Sci* 2016;57(13):5200-06. doi: 10.1167/iovs.16-19964
- S134. Gulshan V, Peng L, Coram M, et al. Development and Validation of a Deep Learning Algorithm for Detection of Diabetic Retinopathy in Retinal Fundus Photographs. *JAMA* 2016;316(22):2402-10. doi: 10.1001/jama.2016.17216
- S135. Gargeya R, Leng T. Automated Identification of Diabetic Retinopathy Using Deep Learning. *Ophthalmology* 2017;124(7):962-69. doi: 10.1016/j.ophtha.2017.02.008
- S136. Li Z, Keel S, Liu C, et al. An Automated Grading System for Detection of Vision-Threatening Referable Diabetic Retinopathy on the Basis of Color Fundus Photographs. *Diabetes Care* 2018 doi: 10.2337/dc18-0147
- S137. Kanagasingam Y, Xiao D, Vignarajan J, et al. Evaluation of Artificial Intelligence-Based Grading of Diabetic Retinopathy in Primary Care. *JAMA Netw Open* 2018;1(5):e182665. doi: 10.1001/jamanetworkopen.2018.2665
- S138. Burlina PM, Joshi N, Pacheco KD, et al. Assessment of Deep Generative Models for High-Resolution Synthetic Retinal Image Generation of Age-Related Macular Degeneration. *JAMA Ophthalmol* 2019;137(3):258-64. doi: 10.1001/jamaophthalmol.2018.6156
- S139. Peng Y, Dharssi S, Chen Q, et al. DeepSeeNet: A Deep Learning Model for Automated Classification of Patient-based Age-related Macular Degeneration Severity from Color Fundus Photographs. *Ophthalmology* 2019;126(4):565-75. doi: 10.1016/j.ophtha.2018.11.015
- S140. Burlina PM, Joshi N, Pacheco KD, et al. Use of Deep Learning for Detailed Severity Characterization and Estimation of 5-Year Risk Among Patients With Age-Related

- Macular Degeneration. *JAMA Ophthalmol* 2018;136(12):1359-66. doi: 10.1001/jamaophthalmol.2018.4118
- S141. Li Z, He Y, Keel S, et al. Efficacy of a Deep Learning System for Detecting Glaucomatous Optic Neuropathy Based on Color Fundus Photographs. *Ophthalmology* 2018;125(8):1199-206. doi: 10.1016/j.ophtha.2018.01.023
- S142. Medeiros FA, Jammal AA, Thompson AC. From Machine to Machine: An OCT-Trained Deep Learning Algorithm for Objective Quantification of Glaucomatous Damage in Fundus Photographs. *Ophthalmology* 2019;126(4):513-21. doi: 10.1016/j.ophtha.2018.12.033
- S143. Redd TK, Campbell JP, Brown JM, et al. Evaluation of a deep learning image assessment system for detecting severe retinopathy of prematurity. *Br J Ophthalmol* 2018 doi: 10.1136/bjophthalmol-2018-313156
- S144. Brown JM, Campbell JP, Beers A, et al. Automated Diagnosis of Plus Disease in Retinopathy of Prematurity Using Deep Convolutional Neural Networks. *JAMA Ophthalmol* 2018;136(7):803-10. doi: 10.1001/jamaophthalmol.2018.1934
- S145. Kermany DS, Goldbaum M, Cai W, et al. Identifying Medical Diagnoses and Treatable Diseases by Image-Based Deep Learning. *Cell* 2018;172(5):1122-31 e9. doi: 10.1016/j.cell.2018.02.010
- S146. Schlegl T, Waldstein SM, Bogunovic H, et al. Fully Automated Detection and Quantification of Macular Fluid in OCT Using Deep Learning. *Ophthalmology* 2018;125(4):549-58. doi: 10.1016/j.ophtha.2017.10.031
- S147. De Fauw J, Ledsam JR, Romera-Paredes B, et al. Clinically applicable deep learning for diagnosis and referral in retinal disease. *Nat Med* 2018;24(9):1342-50. doi: 10.1038/s41591-018-0107-6
- S148. Ran AR, Cheung CY, Wang X, et al. Detection of glaucomatous optic neuropathy with spectral-domain optical coherence tomography: a retrospective training and validation deep-learning analysis. *The Lancet Digital Health* 2019;1(4):e172-e82. doi: 10.1016/S2589-7500(19)30085-8
- S149. Wagner SK, Fu DJ, Faes L, et al. Insights into Systemic Disease through Retinal Imaging-Based Oculomics. *Translational Vision Science & Technology* 2020;9(2):6-6. doi: 10.1167/tvst.9.2.6
- S150. Dumitrascu OM, Koronyo-Hamaoui M. Retinal vessel changes in cerebrovascular disease. *Curr Opin Neurol* 2020;33(1):87-92. doi: 10.1097/WCO.0000000000000779

- S151. Shi L, Baird AL, Westwood S, et al. A Decade of Blood Biomarkers for Alzheimer's Disease Research: An Evolving Field, Improving Study Designs, and the Challenge of Replication. *J Alzheimers Dis* 2018;62(3):1181-98. doi: 10.3233/JAD-170531
- S152. Nakamura A, Kaneko N, Villemagne VL, et al. High performance plasma amyloid-beta biomarkers for Alzheimer's disease. *Nature* 2018;554(7691):249-54. doi: 10.1038/nature25456
- S153. Campbell M, Humphries P. The blood-retina barrier: tight junctions and barrier modulation. *Adv Exp Med Biol* 2012;763:70-84.
- S154. Patton N, Aslam T, Macgillivray T, et al. Retinal vascular image analysis as a potential screening tool for cerebrovascular disease: a rationale based on homology between cerebral and retinal microvasculatures. *J Anat* 2005;206(4):319-48.
- S155. Holash JA, Stewart PA. The relationship of astrocyte-like cells to the vessels that contribute to the blood-ocular barriers. *Brain Res* 1993;629(2):218-24.
- S156. Hawkins BT, Davis TP. The blood-brain barrier/neurovascular unit in health and disease. *Pharmacol Rev* 2005;57(2):173-85. doi: 10.1124/pr.57.2.4
- S157. Iadecola C. The Neurovascular Unit Coming of Age: A Journey through Neurovascular Coupling in Health and Disease. *Neuron* 2017;96(1):17-42. doi: 10.1016/j.neuron.2017.07.030
- S158. Pournaras CJ, Rungger-Brandle E, Riva CE, et al. Regulation of retinal blood flow in health and disease. *Prog Retin Eye Res* 2008;27(3):284-330. doi: 10.1016/j.preteyeres.2008.02.002
- S159. Crowe MJ, Bresnahan JC, Shuman SL, et al. Apoptosis and delayed degeneration after spinal cord injury in rats and monkeys. *Nat Med* 1997;3(1):73-6.
- S160. Levkovitch-Verbin H, Quigley HA, Kerrigan-Baumrind LA, et al. Optic nerve transection in monkeys may result in secondary degeneration of retinal ganglion cells. *Invest Ophthalmol Vis Sci* 2001;42(5):975-82.
- S161. Levkovitch-Verbin H, Quigley HA, Martin KR, et al. A model to study differences between primary and secondary degeneration of retinal ganglion cells in rats by partial optic nerve transection. *Invest Ophthalmol Vis Sci* 2003;44(8):3388-93.
- S162. So KF, Yip HK. Regenerative capacity of retinal ganglion cells in mammals. *Vision Res* 1998;38(10):1525-35. doi: 10.1016/s0042-6989(97)00226-5
- S163. Streilein JW. Ocular immune privilege: therapeutic opportunities from an experiment of nature. *Nat Rev Immunol* 2003;3(11):879-89. doi: 10.1038/nri1224

- S164. Kaur C, Foulds WS, Ling EA. Blood-retinal barrier in hypoxic ischaemic conditions: basic concepts, clinical features and management. *Prog Retin Eye Res* 2008;27(6):622-47. doi: 10.1016/j.preteyeres.2008.09.003
- S165. Schuetz E, Thanos S. Neuro-glial interactions in the adult rat retina after reaxotomy of ganglion cells: examination of neuron survival and phagocytic microglia using fluorescent tracers. *Brain Res Bull* 2004;62(5):391-6. doi: 10.1016/j.brainresbull.2003.10.008
- S166. Mato M, Ookawara S, Sakamoto A, et al. Involvement of specific macrophage-lineage cells surrounding arterioles in barrier and scavenger function in brain cortex. *Proc Natl Acad Sci U S A* 1996;93(8):3269-74.
- S167. Farkas E, Luiten PG. Cerebral microvascular pathology in aging and Alzheimer's disease. *Prog Neurobiol* 2001;64(6):575-611.
- S168. Hoste AM, Boels PJ, Andries LJ, et al. Effects of beta-antagonists on contraction of bovine retinal microarteries in vitro. *Invest Ophthalmol Vis Sci* 1990;31(7):1231-7.
- S169. Laties AM. Central retinal artery innervation. Absence of adrenergic innervation to the intraocular branches. *Arch Ophthalmol* 1967;77(3):405-9.
- S170. Huang D, Swanson EA, Lin CP, et al. Optical coherence tomography. *Science* 1991;254(5035):1178-81.
- S171. Adhi M, Liu JJ, Qavi AH, et al. Choroidal analysis in healthy eyes using swept-source optical coherence tomography compared to spectral domain optical coherence tomography. *Am J Ophthalmol* 2014;157(6):1272-81 e1. doi: 10.1016/j.ajo.2014.02.034
- S172. Mrejen S, Spaide RF. Optical coherence tomography: imaging of the choroid and beyond. *Surv Ophthalmol* 2013;58(5):387-429. doi: 10.1016/j.survophthal.2012.12.001
- S173. Mwanza JC, Oakley JD, Budenz DL, et al. Macular ganglion cell-inner plexiform layer: automated detection and thickness reproducibility with spectral domain-optical coherence tomography in glaucoma. *Invest Ophthalmol Vis Sci* 2011;52(11):8323-9. doi: 10.1167/iovs.11-7962
- S174. Stanga PE, Tsamis E, Papayannis A, et al. Swept-Source Optical Coherence Tomography Angio (Topcon Corp, Japan): Technology Review. *Dev Ophthalmol* 2016;56:13-7. doi: 10.1159/000442771
- S175. Wang RK, An L, Francis P, et al. Depth-resolved imaging of capillary networks in retina and choroid using ultrahigh sensitive optical microangiography. *Opt Lett* 2010;35(9):1467-9. doi: 10.1364/OL.35.001467

- S176. Coscas F, Sellam A, Glacet-Bernard A, et al. Normative Data for Vascular Density in Superficial and Deep Capillary Plexuses of Healthy Adults Assessed by Optical Coherence Tomography Angiography. *Invest Ophthalmol Vis Sci* 2016;57(9):OCT211-23. doi: 10.1167/iovs.15-18793
- S177. Durbin MK, An L, Shemonski ND, et al. Quantification of Retinal Microvascular Density in Optical Coherence Tomographic Angiography Images in Diabetic Retinopathy. *JAMA Ophthalmol* 2017;135(4):370-76. doi: 10.1001/jamaophthalmol.2017.0080
- S178. Spaide RF, Fujimoto JG, Waheed NK. Image Artifacts in Optical Coherence Tomography Angiography. *Retina* 2015;35(11):2163-80. doi: 10.1097/IAE.0000000000000765
- S179. Spaide RF, Koizumi H, Pozzoni MC. Enhanced depth imaging spectral-domain optical coherence tomography. *Am J Ophthalmol* 2008;146(4):496-500. doi: 10.1016/j.ajo.2008.05.032
- S180. Gupta P, Jing T, Marziliano P, et al. Peripapillary choroidal thickness assessed using automated choroidal segmentation software in an Asian population. *Br J Ophthalmol* 2015;99(7):920-6. doi: 10.1136/bjophthalmol-2014-306152
- S181. Agrawal R, Gupta P, Tan KA, et al. Choroidal vascularity index as a measure of vascular status of the choroid: Measurements in healthy eyes from a population-based study. *Sci Rep* 2016;6:21090. doi: 10.1038/srep21090
- S182. Agrawal R, Ding J, Sen P, et al. Exploring choroidal angioarchitecture in health and disease using choroidal vascularity index. *Prog Retin Eye Res* 2020:100829. doi: 10.1016/j.preteyeres.2020.100829
- S183. Hubbard LD, Brothers RJ, King WN, et al. Methods for evaluation of retinal microvascular abnormalities associated with hypertension/sclerosis in the Atherosclerosis Risk in Communities Study. *Ophthalmology* 1999;106(12):2269-80.
- S184. Wong TY, Knudtson MD, Klein R, et al. Computer-assisted measurement of retinal vessel diameters in the Beaver Dam Eye Study: methodology, correlation between eyes, and effect of refractive errors. *Ophthalmology* 2004;111(6):1183-90.
- S185. Knudtson MD, Lee KE, Hubbard LD, et al. Revised formulas for summarizing retinal vessel diameters. *Curr Eye Res* 2003;27(3):143-49.
- S186. Cheung CY, Tay WT, Mitchell P, et al. Quantitative and Qualitative Retinal Microvascular Characteristics and Blood Pressure. *J Hypertens* 2011
- S187. Garhofer G, Bek T, Boehm AG, et al. Use of the retinal vessel analyzer in ocular blood flow research. *Acta Ophthalmol* 2010;88(7):717-22. doi: 10.1111/j.1755-3768.2009.01587.x

- S188. Hirano T, Imai A, Kasamatsu H, et al. Assessment of diabetic retinopathy using two ultra-wide-field fundus imaging systems, the Clarus(R) and Optos systems. *BMC Ophthalmol* 2018;18(1):332. doi: 10.1186/s12886-018-1011-z
- S189. Kernt M, Hadi I, Pinter F, et al. Assessment of diabetic retinopathy using nonmydriatic ultra-widefield scanning laser ophthalmoscopy (Optomap) compared with ETDRS 7-field stereo photography. *Diabetes Care* 2012;35(12):2459-63. doi: 10.2337/dc12-0346
- S190. Silva PS, Cavallerano JD, Haddad NM, et al. Peripheral Lesions Identified on Ultrawide Field Imaging Predict Increased Risk of Diabetic Retinopathy Progression over 4 Years. *Ophthalmology* 2015;122(5):949-56. doi: 10.1016/j.ophtha.2015.01.008
- S191. Lengyel I, Csutak A, Florea D, et al. A Population-Based Ultra-Widefield Digital Image Grading Study for Age-Related Macular Degeneration-Like Lesions at the Peripheral Retina. *Ophthalmology* 2015;122(7):1340-7. doi: 10.1016/j.ophtha.2015.03.005
- S192. Dysli C, Quelled G, Abegg M, et al. Quantitative analysis of fluorescence lifetime measurements of the macula using the fluorescence lifetime imaging ophthalmoscope in healthy subjects. *Invest Ophthalmol Vis Sci* 2014;55(4):2106-13. doi: 10.1167/iovs.13-13627
- S193. Larrosa JM, Garcia-Martin E, Bambo MP, et al. Potential new diagnostic tool for Alzheimer's disease using a linear discriminant function for Fourier domain optical coherence tomography. *Invest Ophthalmol Vis Sci* 2014;55(5):3043-51. doi: 10.1167/iovs.13-13629
- S194. Polo V, Garcia-Martin E, Bambo MP, et al. Reliability and validity of Cirrus and Spectralis optical coherence tomography for detecting retinal atrophy in Alzheimer's disease. *Eye (Lond)* 2014;28(6):680-90. doi: 10.1038/eye.2014.51
- S195. Ferrari L, Huang SC, Magnani G, et al. Optical Coherence Tomography Reveals Retinal Neuroaxonal Thinning in Frontotemporal Dementia as in Alzheimer's Disease. *J Alzheimers Dis* 2017;56(3):1101-07. doi: 10.3233/JAD-160886
- S196. Garcia-Martin E, Bambo MP, Marques ML, et al. Ganglion cell layer measurements correlate with disease severity in patients with Alzheimer's disease. *Acta Ophthalmol* 2016;94(6):e454-9. doi: 10.1111/aos.12977
- S197. Cunha JP, Proenca R, Dias-Santos A, et al. OCT in Alzheimer's disease: thinning of the RNFL and superior hemiretina. *Graefes Arch Clin Exp Ophthalmol* 2017;255(9):1827-35. doi: 10.1007/s00417-017-3715-9
- S198. Asanad S, Fantini M, Sultan W, et al. Retinal nerve fiber layer thickness predicts CSF amyloid/tau before cognitive decline. *PLoS One* 2020;15(5):e0232785. doi: 10.1371/journal.pone.0232785

- S199. McCann P, Hogg R, Wright DM, et al. Intraocular pressure and circumpapillary retinal nerve fibre layer thickness in the Northern Ireland Cohort for the Longitudinal Study of Ageing (NICOLA): distributions and associations. *Br J Ophthalmol* 2020 doi: 10.1136/bjophthalmol-2020-316499
- S200. Santos CY, Johnson LN, Sinoff SE, et al. Change in retinal structural anatomy during the preclinical stage of Alzheimer's disease. *Alzheimers Dement (Amst)* 2018;10:196-209. doi: 10.1016/j.dadm.2018.01.003
- S201. Lee JY, Kim JP, Jang H, et al. Optical coherence tomography angiography as a potential screening tool for cerebral small vessel diseases. *Alzheimers Res Ther* 2020;12(1):73. doi: 10.1186/s13195-020-00638-x

